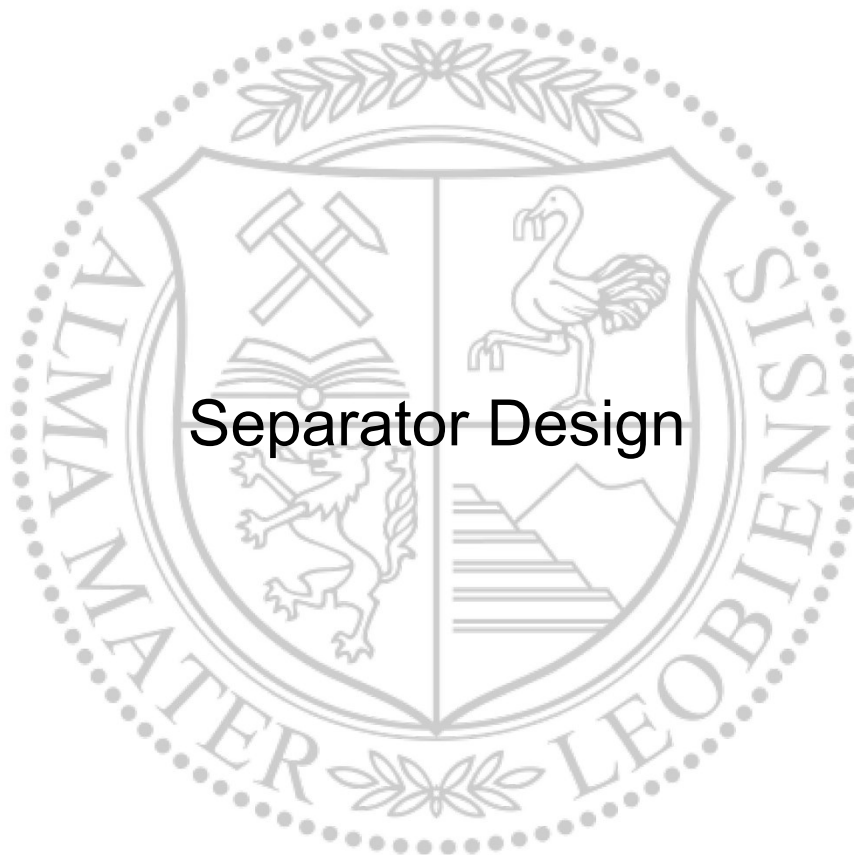




Chair of Petroleum and Geothermal Energy Recovery

Master's Thesis



Separator Design

Christoph Martin Flicker, BSc

May, 2019

**EIDESSTATTLICHE ERKLÄRUNG**

Ich erkläre an Eides statt, dass ich diese Arbeit selbständig verfasst, andere als die angegebenen Quellen und Hilfsmittel nicht benutzt, und mich auch sonst keiner unerlaubten Hilfsmittel bedient habe.

Ich erkläre, dass ich die Richtlinien des Senats der Montanuniversität Leoben zu "Gute wissenschaftliche Praxis" gelesen, verstanden und befolgt habe.

Weiters erkläre ich, dass die elektronische und gedruckte Version der eingereichten wissenschaftlichen Abschlussarbeit formal und inhaltlich identisch sind.

Datum 19.05.2019

A handwritten signature in blue ink that reads "Flicker".

Unterschrift Verfasser/in
Christoph Martin, Flicker
Matrikelnummer: 01335201

Kurzfassung

Eine Kette ist nur so stark wie ihr schwächstes Glied und dasselbe gilt auch für die Mineralölindustrie mit ihren Upstream-, Midstream- und Downstream-Sektoren. Jeder Prozess im gesamten Zyklus muss vollständig verstanden werden, um ihn so weit wie möglich zu optimieren. Im Rahmen dieses Projektes wurden die Entwurfs- und Auslegungsprozesse von Öl- und Gasseparatoren untersucht, die das geförderte Gemisch in Wasser, Öl und Gas trennen, und die finale Komponente des sogenannten Erdölproduktionssystems darstellen.

Diese Masterarbeit dient als Erklärung und Leitfaden für die Auslegung eines Separators. Labormessungen und Analyse des Phasenverhaltens zur Bestimmung der Charakteristika, Zusammensetzung und Eigenschaften des Rohöls, die zu einem späteren Zeitpunkt als entscheidende Eingabeparameter dienen, sind der erste Schritt und werden daher ausführlich erläutert. Darüber hinaus werden die Auswahl des grundlegenden Separatortyps und die Behälterkonfiguration für die vorhandene Anzahl der Phasen, die richtige Anwendung und die Betriebsbedingungen empfohlen. Anschließend werden die vier Funktionsabschnitte in einem Separator dargestellt und die Gleichungen, die die Physik hinter den Zwei- und Dreiphasentrennvorgängen beschreiben, werden zum besseren Verständnis vollständig hergeleitet. Die Beschreibung der Dimensionierung selbst, die auf den Theorien der Tropfenabscheidung und den Retentionszeiten basiert und viele Eingabeparameter und vorgegebene Werte erfordert, führt zu den endgültigen Abmessungen des Druckbehälters und den geeigneten Gas- und Flüssigkeitskapazitäten. Um möglichen Problemen vorzubeugen, sie zu vermeiden und ihnen entgegenzuwirken, wird die Vielfalt der möglichen Einbauten dargestellt und erklärt. Die Anforderungen in Bezug auf Gesundheit, Sicherheit und Umwelt (GSU) und die American Society of Mechanical Engineers (ASME) wurden ebenfalls analysiert und berücksichtigt.

Eine numerische Strömungsdynamiksimulation eines horizontalen Dreiphasenseparators mit einigen Einbauten wurde in OpenFOAM durchgeführt und wird am Ende der Masterarbeit vorgestellt. Dabei wurde ein Multiphasenlöser für inkompressible und komprimierbare Phasen verwendet, dessen Einsatz für Separatoren bisher noch in keiner Literatur beschrieben wurde. Die Geometrie und das Mesh-Gitter wurden in den Geometrie- und Mesh-Modulen von SALOME erstellt, während die Nachbearbeitung in ParaView zu Visualisierungszwecken durchgeführt wurde.

Abstract

A chain is only as strong as its weakest link and the same counts for the petroleum industry with its upstream, midstream and downstream sectors. Every process in the entire lifecycle has to be fully understood in order to optimize it as much as possible. Within that project, the design and sizing of oil and gas separators, which represent the last component of the so-called petroleum production system, have been examined.

This thesis is an explanation and a guideline for the design of a separator from scratch. Laboratory measurements and pressure volume temperature (PVT) analysis to determine the characteristics, composition and fluid properties of the crude petroleum, which are crucial input parameters at a later stage, are the first step and hence are explained in detail. Further, the basic separator type selection and vessel configuration for the present number of phases, right application and operating conditions is advised. The four functional sections in a separator are then illustrated and the equations, which describe the physics behind the phase separation processes, are fully derived for a better understanding. The description of the sizing itself, which is based on the droplet settling theory and retention times, results in the final dimensions of the pressure vessel and the appropriate gas and liquid capacities. To prevent, avoid and counteract any possibly occurring issues, the wide variety of internals is presented and explained. Health, safety and environment (HSE) and American Society of Mechanical Engineers (ASME) requirements have been analyzed and considered as well.

A computational fluid dynamics (CFD) simulation of a horizontal three-phase separator with some internals has been done in OpenFOAM and is presented at the end of the thesis. Within that, a multiphase solver for incompressible and compressible phases has been used, which has not been found for separators in the literature up to this point. Geometry and mesh grid have been created in SALOME while the post-processing has been done in ParaView for visualization purposes.

Table of Content

	Page
1 INTRODUCTION.....	1
1.1 Energy Outlook	1
1.2 Problem Statement	3
1.3 Petroleum Production System.....	3
2 CHARACTERISTICS OF CRUDE PETROLEUM.....	6
2.1 Composition	6
2.2 Classification of Reservoir Fluids	8
2.3 Hydrocarbon Phase Behavior	8
3 SEPARATORS	24
3.1 Definition	24
3.2 Types	24
3.3 Phase Separation	27
3.4 Set-Up.....	31
4 SEPARATOR PERFORMANCE.....	38
4.1 Issues	38
4.2 Efficiency Control	41
5 SEPARATOR SIZING.....	42
5.1 Operating Conditions	42
5.2 General Approach – Half-full Cylindrical Horizontal Three-Phase Separator	43
5.3 API Specification and ASME Code	50
6 HSE.....	52
6.1 Safety Elements.....	52
6.2 Waste Management.....	52
7 COMPUTATIONAL FLUID DYNAMICS MODELING.....	54
7.1 Analytical Calculation.....	54
7.2 Numerical Approach	57
8 CONCLUSION	64
REFERENCES	66
LIST OF TABLES	67

LIST OF FIGURES	68
ABBREVIATIONS	70

1 Introduction

Does petroleum engineering have a chance of survival and still a justification for existence? Many people in the oil and gas industry are already bored by this question, however, even more take it seriously and try to find answers for third parties and themselves. In both cases, it is important to develop the petroleum industry further, either to prove doubters wrong or to avert the end of the hydrocarbon era. Furthermore, it is worth mentioning that it will rather be the overtaking of renewable energies and policies against fossil fuels because of CO₂ emission, than running out of hydrocarbons. Therefore, it is even more crucial to enhance our technologies, decrease the environmental footprint and increase the efficiency in order to stay competitive.

1.1 Energy Outlook

World population growth, ascending urbanization rates and more economic activities are the most important driving forces behind the rising energy consumption and demand. An expected increase of 1.808 billion people from 7.348 billion in 2015 to 9.156 billion in 2040, as shown in Table 1, is mainly ascribable to an increased expectation of life all over the planet. Only 116 million will be contributed by the 35 states of the Organization for Economic Co-operation and Development (OECD) though, while the bulk comes from developing countries, which are obviously no members of the OECD. [1, p. 7]

Table 1: World Population in Millions [1, p. 7]

	Levels				Growth
	2015	2020	2030	2040	2015–2040
OECD	1,280	1,313	1,363	1,397	116
Non-OECD	6,068	6,444	7,137	7,759	1,692
World	7,348	7,757	8,500	9,156	1,808

Growth of cities due to domestic migration and more business-related actions and movement in general, being the other important factors for increasing energy consumption, can and will also be found rather in developing countries. The reason for that is simply the higher remaining potential, which is already exploited to a greater extent in higher developed regions. A gain of 95.6 mboe/d until 2040, as highlighted in Table 2, depicts an increase in energy demand of 35% in total or annually 1.2%. These numbers are composed of 0.1%/year in OECD countries and 1.9%/year in developing countries, with India and China being the largest consumers. [1, p. 9]

Table 2: World Energy Demand in mboe/d [1, p. 9]

	2015	2020	2030	2040
OECD	110.0	113.5	113.6	112.0
Non-OECD	166.0	184.7	225.8	259.6
Total world	276.0	298.2	339.4	371.6

Despite the fact that renewable energies are undoubtedly on the upgrade, fossil fuels will remain the dominant energy sources. Natural gas, being the fastest growing energy source from prehistoric organism, will overtake coal, being the slowest, as highlighted in Table 3. The former will make up together with oil a share of 52.2% in 2040, compared to its 52.8% in 2015 and therefore will still play a major role, especially in non-OECD countries. [1, p. 66]

Table 3: World Energy Demand by Fuel Type [1, p. 66]

	Levels <i>mboe/d</i>				Growth <i>% p.a.</i>	Fuel shares <i>%</i>			
	2015	2020	2030	2040		2015	2020	2030	2040
Oil	86.5	92.3	97.9	100.7	0.6	31.3	30.9	28.8	27.1
Coal	78.0	80.7	85.8	86.2	0.4	28.3	27.0	25.3	23.2
Gas	59.2	65.2	79.9	93.2	1.8	21.5	21.9	23.5	25.1
Nuclear	13.5	15.8	20.1	23.8	2.3	4.9	5.3	5.9	6.4
Hydro	6.8	7.5	9.0	10.3	1.7	2.5	2.5	2.6	2.8
Biomass	28.0	30.1	34.0	37.3	1.2	10.1	10.1	10.0	10.0
Other renewables	3.8	6.6	12.9	20.0	6.8	1.4	2.2	3.8	5.4
Total	276.0	298.2	339.4	371.6	1.2	100	100	100	100

On the other side, this forecasted demand of oil and gas of course needs to be supplied by the industry from hopefully sufficiently existing and available quantities of hydrocarbons. As diagramed in Figure 1, in 2017, the reserves to production ratio was still 50.2 years for oil and 52.6 years for gas, with respectively proven reserves of 1696.6 billion barrels and 193.5 tcm. [2]

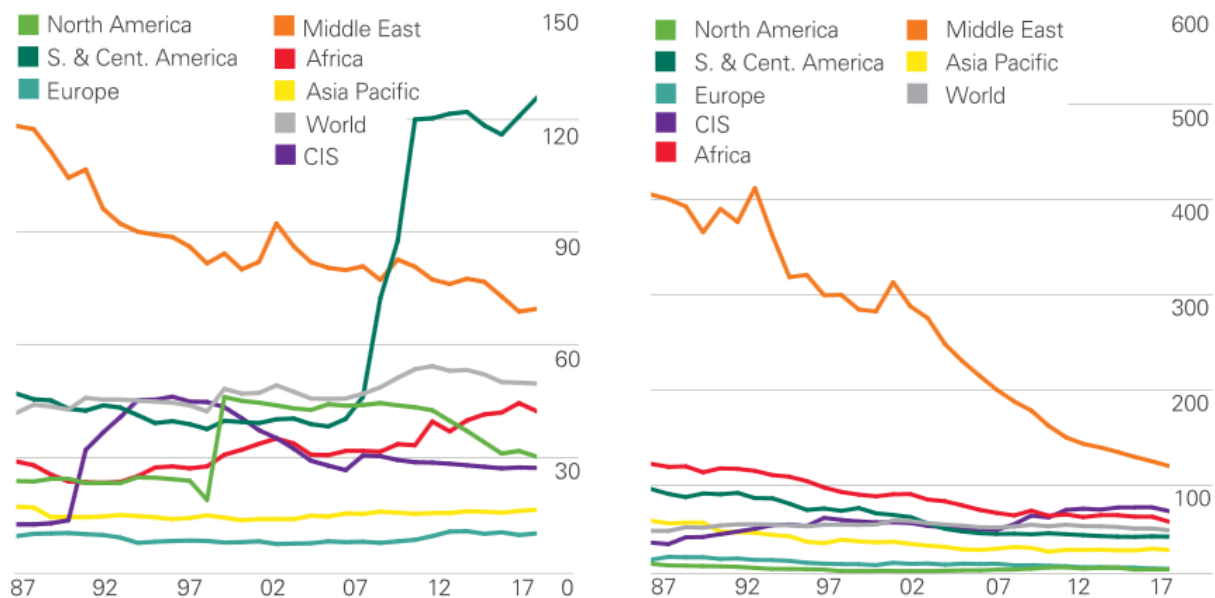


Figure 1: Reserves to Production Ratios over the Last Years (Oil left and Gas right) [2]

1.2 Problem Statement

The well-known slogan Crap In = Crap Out might apply to almost everything in our much digitalized world by now and it is definitely something of which everyone should be aware of even though it rather applies to virtual than physical input. However, bringing the best out of something default and already specified is known as being efficient and this is at least equally crucial. Maximizing the efficiency to keep losses low in terms of time or money, or in other words, develop the quantity and quality of an output to the maximum, should always be the ambition. Especially in the oil and gas industry, optimization procedures in the petroleum production system, which is explained in chapter 1.3, are substantial and hence always leave potential for research and improvement.

Even today, the focus is more on increasing the production rather than efficiently processing the present yield. The understanding of the criteria, requirements and challenges of separators in the oil and gas industry as well as their design and sizing processes are frequently considered as less important. Lack of knowledge about the physics, which underlie the separation processes, and absent computational fluid dynamics simulations definitely have to be made up for. Therefore, a guideline for the entire selection and design procedure of oil and gas separators has been developed throughout this thesis.

1.3 Petroleum Production System

Petroleum has been through many travelling, storing and transformation processes, in short, it has a very long background before humans intentionally encounter the mature solid, liquid and gaseous forms of hydrocarbons by means of a wellbore within a reservoir. Latter is already the first stage of a so-called petroleum production system, which describes the entire closed system through which the petroleum flows during extraction and which can be seen in Figure 2.

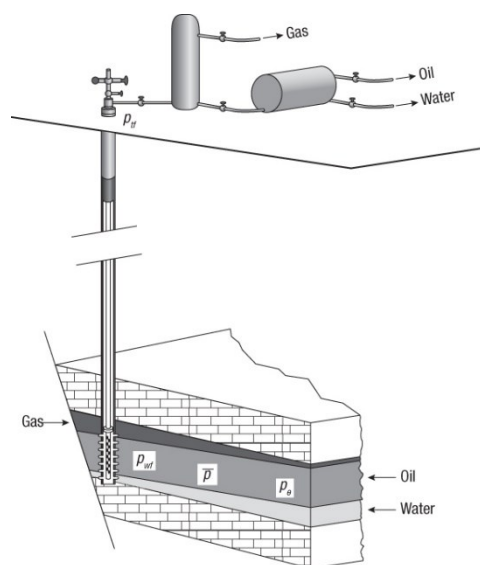


Figure 2: Petroleum Production System [3, p. 12]

1.3.1 Reservoir

In petroleum engineering and its related disciplines, a reservoir is usually defined as a sedimentary rock formation, typically sandstone or carbonate, with sufficient porosity and permeability to store and transmit mature hydrocarbons. However, this actually applies only to conventional reservoirs, which are part of a so-called petroleum system, not to be confused with the petroleum production system. The theory of a petroleum system firstly comprises the presence of a source rock, where mature hydrocarbons are generated out of sedimentary organic matter, called kerogen, after a sufficient amount of time under certain temperature and pressure conditions during diagenesis, catagenesis and metagenesis. The exact temperature and pressure conditions of course slightly vary, however, a typical oil and gas window, which represents the required formation conditions, is shown in Figure 3. Petroleum in a liquid state is usually called crude oil, in a gaseous state natural gas while the so-called condensate can take liquid, gaseous and solid forms.

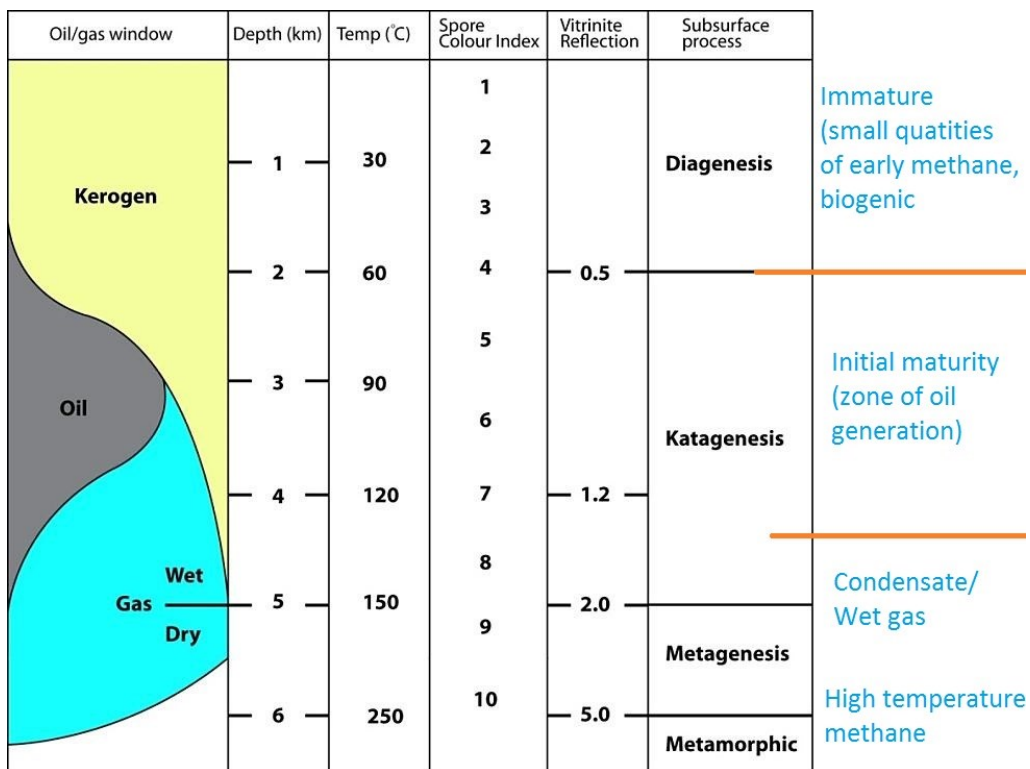


Figure 3: Oil and Gas Window [4]

Secondly, the petroleum movement from the source rock to the reservoir, called migration, and thirdly the trap, formed by a cap or seal rock under which everything is captured and accumulated, and the last element of the petroleum system, the overburden rock. The second category of reservoirs are the so-called unconventional ones, where the source rock simultaneously acts as the reservoir rock due to its low permeability, and where no trap, seal or cap rock is necessary. In both cases, the mature hydrocarbons have to be produced and lifted up to the surface, achieved with the second of three big components of the petroleum production system, the well or wellbore.

1.3.2 Wellbore

As just mentioned, the only connection and conduit between the reservoir in the subsurface and the surface facilities is the well with its constituent parts. The lower completion, being the interface between the reservoir and the wellbore, can be either cemented and cased, open hole, or one of its many variations with different downhole components like a slotted or pre-drilled liner. For sand control, gravel packs or sand screens can also be installed as a part of the lower completion. Passing by this near wellbore zone and entering the well, which definitely brings along the highest pressure drop, then results in a specific bottom hole flowing pressure, p_{wf} . In natural flowing wells, this pressure overcomes the hydrostatic pressure, friction losses and acceleration head, which are described by the so-called Vertical Lift Performance (VLP) or Tubing Performance Relation (TPR) on its way up the tubing. If this is not the case, the fluid has to be lifted either mechanically by energizing the medium with pumps or by decreasing its density by means of gas lift, being the two major types of artificial lift systems. Acceleration head losses occur with compressible fluids or for example at downhole chokes, landing nipples, subsurface safety valves or any other restriction inside the tubing, where the cross section changes.

1.3.3 Surface Equipment

Once the fluid mixture passes by the surface choke, which determines the magnitude of the well flowing pressure by exerting a backpressure on the surface, it flows through the flow lines right into a separator. Separators, which then isolate the various phases for further processing, are the last stage of the upstream sector in the oil and gas industry and the transition to midstream, where the oil and gas is transported towards the downstream entities.

2 Characteristics of Crude Petroleum

In order to design and select the appropriate equipment, it is crucial to know the composition, characteristics and properties of the present media. Furthermore, one has to be aware of the fact that the reservoir fluid changes during reservoir depletion and also during the uplift process due to changing pressure and temperature conditions. The ideal case of a monophasic reservoir fluid is seldom or never given but rather an emulsion, where two liquid phases are somehow mixed, a suspension, where solid particles are distributed in a fluid phase, or something foamy, which is the result of a mix of a gaseous and liquid phase. Details of those issues and how to fight against these mixtures of two, three or even four phases are shown in chapter 4.1 later on.

2.1 Composition

Crude petroleum, independently of its state, is mainly composed of hydrocarbons as shown by the typical oil composition in Figure 4, with an emphasis on mainly. However, as the name already indicates, hydrocarbons itself are chemical compounds composed only of carbon and hydrogen in a gaseous, liquid and sometimes solid state depending on the composition, temperature and pressure conditions. Generally, they can be classified into two major groups, namely the aliphatic and aromatic compounds. For the classification of crude petroleum though, which consists not only of hydrocarbon compounds but also of other organic compounds, a third group called the heterocyclic compounds, is usually added as shown in Figure 5. This class of substances also contains atoms other than carbon and hydrogen. [5, pp. 269-270]

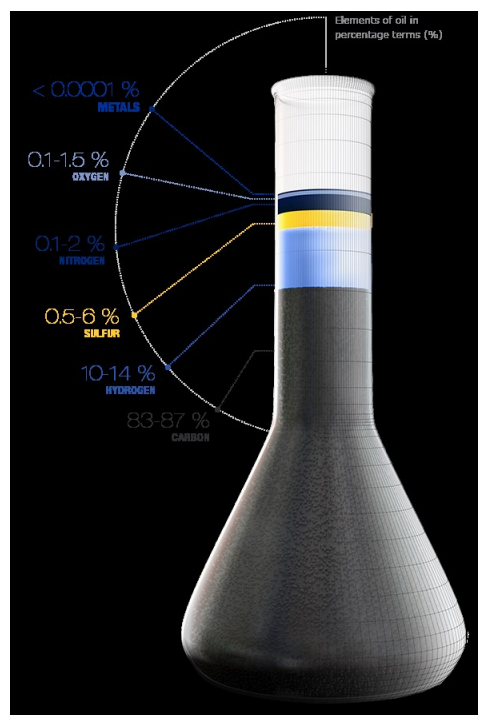


Figure 4: Elements of Crude Oil in Percentage [6]

2.1.1 Aliphatic Hydrocarbons

Aliphatic hydrocarbons can then be subdivided into saturated and unsaturated hydrocarbons as shown in the already mentioned Figure 5. The former either have a chain-structure and bear the name alkanes or paraffins, or a ring-structure which are then called cycloalkanes, cycloparaffins or simply naphthenes. Paraffins can be described by the chemical formula C_nH_{2n+2} , with n being the number of carbon atoms and have only single bonds while cycloalkanes are described by the formula C_nH_{2n} . Especially natural gas is mainly made up of CH_4 , called methane, the simplest representative of alkanes. Additionally, it is also important to distinguish between normal and iso alkanes, short, n - and i -alkanes. Latter are called isomers, which have the same structural formula but a different geometry that leads to other characteristics and properties. With increasing number of carbon atoms and hence bigger molecules, the number of possible isomers raises and this is already the explanation for the intricacy of oil compared to the simplicity of gas. Unsaturated hydrocarbons with double bonds are called alkenes or olefins, ones with triple bonds bear the name alkynes. However, they are not as common as the saturated ones. [5, pp. 270-271]

2.1.2 Aromatic Hydrocarbons

Organic compounds with double bonds, and hence unsaturated hydrocarbons, and a cyclic structure can be represented by the formula C_nH_{2n-6} and are called aromatics. The simplest representative Benzene, C_6H_6 , with its three alternating double bonds, is the basal of these ring-structured, sweet and well smelling compounds. [5, p. 272]

2.1.3 Heterocyclic Compounds

Despite the fact that petroleum primarily consists of hydrocarbons, other compounds like nitrogen, sulphur or oxygen can and actually are present as well. These NSO- or heterocyclic compounds, also depicted in Figure 5, often form very complex structures and are responsible for some conspicuous properties of crude oil or gas like sourness and changes in pseudocritical properties. [5, p. 270]

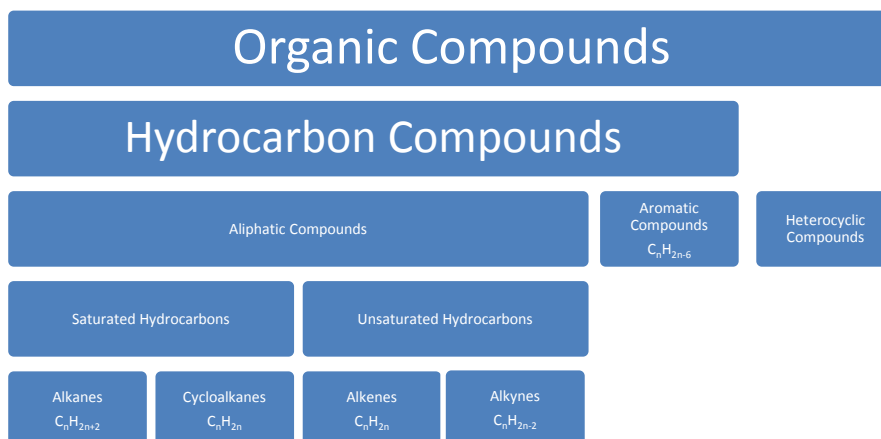


Figure 5: Organic Compounds in Crude Petroleum

2.2 Classification of Reservoir Fluids

As previously mentioned, natural gas' composition is rather simple compared to all the crude oils'. On the one hand, it mainly consists of smaller molecules such as the major constituent methane, some other lighter hydrocarbons, carbon dioxide, hydrogen sulphide and nitrogen. On the other hand, crude oil consists of much larger molecules with more possible isomers, is therefore much more complex and has many different variants. Due to the occurrence of so many several oil types, the specific gravity has been introduced as the primary physical classification ahead of viscosity, color, sulphur content and refractive index. It is defined as the ratio of the oil density and the water density in the same arbitrary unit at standard conditions of 60°F and 14.7 psia, dimensionless and shown in **eq.1** [5, p. 276].

$$\gamma_o = \frac{\rho_o}{\rho_w} \quad (1)$$

This exact specific gravity can then be used in the second most important physical classification of crude oils, the °API or API Gravity in **eq.2** [5, p. 277], established by the American Petroleum Institute.

$$API\ Gravity = \frac{141.5}{Specific\ Gravity} - 131.5 \quad (2)$$

Crude oil with an API grade below 22.3 is usually referred to as heavy, above 31.1 as light and right in between as medium, as summarized in Table 4. Sometimes, the category extra heavy is added with crude oils heavier than water, which has by definition an API gravity of 10. [7]

Table 4: Crude Oil Classification according to °API [7]

Class	°API
Light	>31.1
Medium	>22.3 & <31.1
Heavy	>10 & <22.3
Extra Heavy	<10

2.3 Hydrocarbon Phase Behavior

In order to predict the state of the reservoir fluid in the wellbore and on surface, which is essential for the selection of artificial lift systems and other equipment and very important for the separator design, it is crucial to understand its so-called phase behavior. First of all, it is necessary to clearly define some terms, even though they have been already used on the prior pages. As previously mentioned, petroleum can occur as a single- or multiphase system, with a phase being a homogeneous, physically distinctive part with uniform chemical and physical properties, bounded by a surface. In the case of hydrocarbons, this can be the gaseous, liquid or solid phase, which are either present alone or coexist in equilibrium with one or both of the

others. An equilibrium is referred to as a condition or state, where no mass or heat transfer occurs between the phases and the energy of the system does not change. A component is then a chemically-discrete constituent of a phase or system, which is quantitatively described by the composition, being the portion or share of the component in the entire mixture. [5, p. 286]

The phase behavior is mainly a function of chemistry, composition, pressure and temperature and usually depicted in a pressure-temperature diagram for a given chemistry and overall system composition as shown later on. So as to describe and analyze reservoir fluids, which are mostly multicomponent mixtures, pure components are examined at first.

Further, it is recommended to keep the so-called Gibbs' Phase Rule, as shown in **eq.3** [5, p. 287], at the back of the mind throughout this entire thesis. It basically reveals and calculates the degrees of freedom of a system. Table 5 presents the independent variables necessary to define a system with its different number of phases.

$$F = C - P + 2 \quad (3)$$

Table 5: Gibbs' Phase Rule [5, pp. 287-304]

F = C - P + 2		
C = 1	P = 1	F = 2 (pressure and temperature)
	P = 2	F = 1 (pressure or temperature)
	P = 3	F = 0
C = 2	P = 1	F = 3 (pressure, temperature and composition)
	P = 2	F = 2 (pressure and temperature)
	P = 3	F = 1 (pressure or temperature)

F degrees of freedom [-]

C number of components [-]

P number of phases [-]

2.3.1 Pure Component

In the case of a single component, the p-T diagram exhibits five important characteristics, namely the triple point, critical point, vapor pressure curve, melting point curve and sublimation pressure curve. Former is the converging point of vapor pressure curve, melting point curve and sublimation curve and the only possible pressure and temperature condition where all three phases of the pure component can coexist at equilibrium, as shown in Figure 6. The critical point is defined by its belonging critical pressure p_c and critical temperature T_c beyond distinction between phases is not possible anymore. This state is therefore called supercritical and also highlighted in the subsequent figure as painted areas. [5, pp. 288-290]

Excess of one of these three curves in the pressure-temperature diagram always represents a change from one to another phase. Since a reservoir depletion is mostly approximated by a pressure decline at constant temperature, vertical lines, representing an isothermal pressure decrease, are used for explanation of the phase changes. The vapor pressure curve, with the triple point and the critical point at its ends, represents the equilibrium of the gaseous and liquid phases. During an isothermal pressure decline at a fixed bubble point temperature T_b from point A to point C, the pressure on that vapor pressure curve is called bubble point pressure p_b and highlighted as point B in Figure 6. This exact pressure and the temperature at point B are respectively called dew point pressure and dew point temperature during a pressure increase from point C to point A. Therefore, the vapor pressure curve is the sum of all possible bubble point pressures, where the first bubble liberates from the liquid during evaporation, or dew point pressures at which first liquid droplets precipitate from the gaseous phase during condensation at fixed bubble or dew point temperatures. Furthermore, the almost vertical dashed melting point curve represents the equilibrium between the solid and liquid phases and an excess is either called melting or solidification, depending on the direction. In the end, a transition across the sublimation curve, which symbolizes the equilibrium of the solid and gaseous phases, is referred to as sublimation or deposition, again depending on the direction of the process. [5, pp. 288-290]

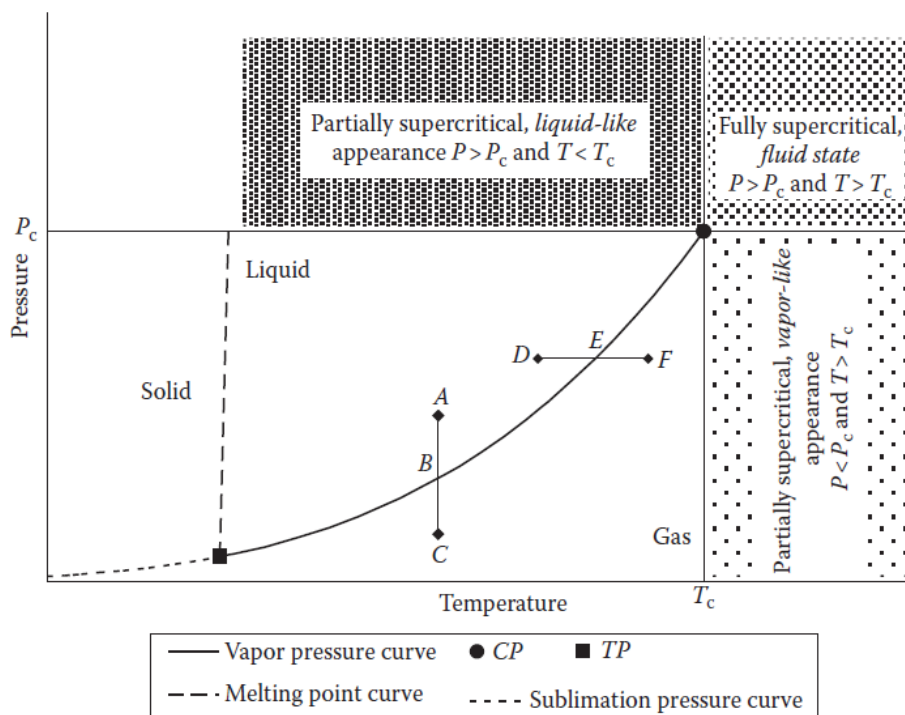


Figure 6: Phase Diagram of a Pure Component [5, p. 288]

2.3.2 Mixture

As the name already indicates, a mixture contains more than one component and so does every reservoir fluid. In general, the definitions of bubble point and dew point retain, however, equilibrium between the two phases is now represented by an area instead of a single curve like the vapor pressure curve for pure components. The bubble point curve, the connection of

bubble point pressures at various bubble point temperatures, and the dew point curve, the line through all dew point pressures at different dew point temperatures, are now separated, converge only in the critical point and enclose a so-called phase envelope or saturation envelope. [5, p. 295]

2.3.2.1 Binary System

Two component or binary systems show some additional features in their phase diagrams. The cricondetherm, determined by a vertical tangent to the phase envelope, and the cricondenbar, ascertained by a horizontal tangent to the two-phase region, respectively illustrate the maximum temperature and pressure where two phases can coexist at equilibrium. In a pure component system, maximum pressure and temperature at which two phases can exist together at equilibrium define the critical point and beyond this point, it cannot be differentiated between the phases. However, in a binary system, there is an area above this point where this is also possible. Only at the critical point and beyond the cricondetherm and cricondenbar, it is not possible to distinguish one phase from another. [5, pp. 295-296]

A depletion as shown by the mark from A to B in Figure 7 firstly encounters the bubble point curve, where gas starts to liberate from the single-phase liquid. Further pressure reduction generally just leads to a bigger portion of vapor in equilibrium with the remaining liquid phase until it is completely vaporized at the dew point P_d . While this depletion crosses the bubble point curve and the dew point curve respectively once, an isothermal pressure reduction at a temperature higher than the critical but lower than the cricondetherm has two intersection points with the dew point line. These points, marked in Figure 7 on line E to F, earn the name upper and lower dew point from the definition of the dew point, which fits with the happenings at both of that states. The single-phase vapor forms first liquid bubbles at the upper or retrograde dew point, which is exactly the opposite behavior compared to the upper intersection of the A to B system at the first intersection. The amount of liquid in equilibrium with the gas phase increases until a maximum point somewhere within the phase envelope but then vaporizes due to low pressure until it is a single-phase vapor once again at the lower or normal dew point. Charting the so-called quality lines or iso-vols, which show the liquid-vapor ratio of the present equilibrium, as for example done in the phase diagram of a gas condensate reservoir fluid in chapter 2.3.2.2 later on, additionally clarifies this process. [5, pp. 295-297]

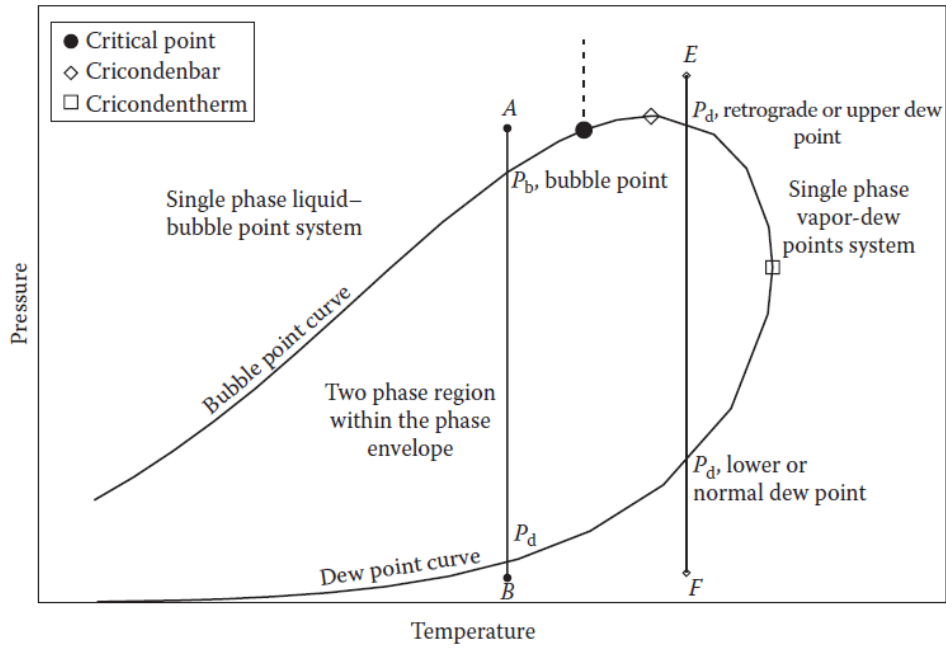


Figure 7: Phase Diagram of a Binary System [5, p. 295]

As previously mentioned, each phase diagram belongs to a specific and fixed overall system composition. Plotting the two-phase areas of various different system compositions and connecting all corresponding critical points, as shown in Figure 8, result in the so-called critical locus. Latter defines the region of a system, regardless of its overall composition, where two phases can coexist in equilibrium. [5, pp. 301-302]

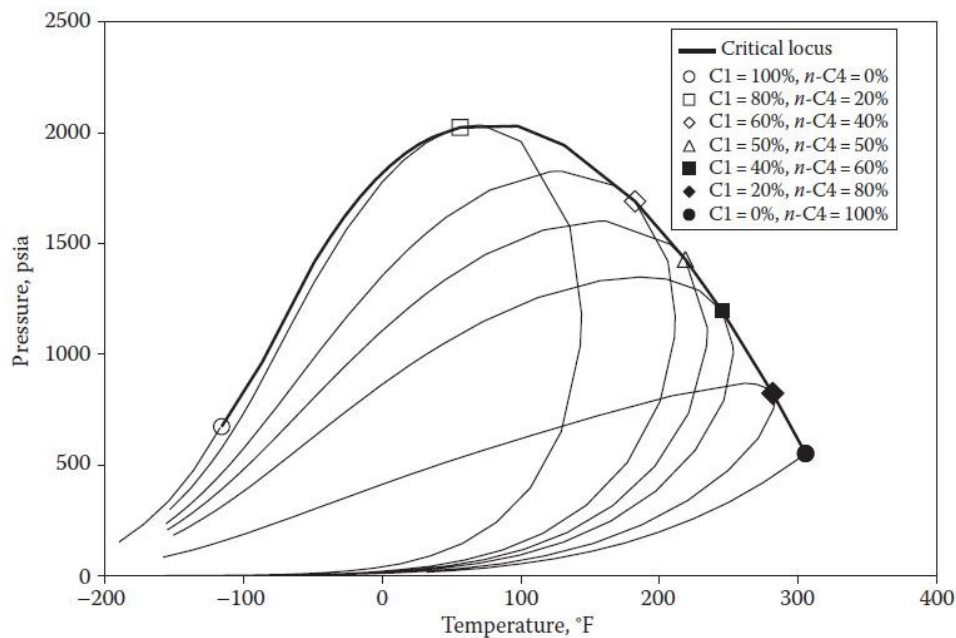


Figure 8: Critical Locus of a Binary System [5, p. 302]

2.3.2.2 Multicomponent System

Practically, every reservoir fluid consists of three or more components and therefore falls into the category of multicomponent systems. In general, the definitions and also the concept remain the same, however, because of the many possible overall compositions, the phase envelopes are mostly only depicted for one specific chemical makeup. Additionally, the two-phase area becomes bigger in terms of pressure and temperature magnitudes compared to a binary system and the critical point shifts to the right. [5, p. 304]

Five different reservoir fluid types are introduced and explained in the subsequent paragraphs in order to describe the different phase behaviors, which can generally occur. A short summary with the main criteria gas oil ratio, gravity, color, plus fraction, formation volume factor and reservoir temperature is shown in Table 6.

Table 6: Classification of Reservoir Fluids [5, p. 314]

Reservoir Fluid	Field Data				Laboratory Analysis		
	Initial Producing GOR (scf/STB)	Initial API Gravity of Liquid	Color of Stock Tank Liquid	Mol% of C ₇₊	Phase Change in Reservoir	Formation Volume Factor (res. bbl/STB)	Reservoir Temperature
Black oil	250–1,750	<45.0	Dark	>20.0	Bubble point	<2.0	<T _c
Volatile oil	1,750–3,200	>40.0	Colored	12.5–20.0	Bubble point	>2.0	<T _c
Gas condensate	>3,200	40.0–60.0	Lightly colored	<12.5	Dew point	—	>T _c
Wet gas	>50,000	Up to 70.0	Water white	May be present in trace amounts	No phase change	—	>Cricondentherm
Dry gas	—	—	—	—	No phase change	—	>Cricondentherm

Black oil has its name from the color at surface conditions and is the most abundant reservoir fluid. On the one hand, the envelope shown on the left in Figure 9, is the biggest of all types; mainly because of a very high critical temperature due to more than 20 mol% of heavy C₇₊ components. On the other hand, these hot conditions lower the bubble point significantly because liberation of gas is favored with increasing temperature. During production and on the way to the surface when the pressure drops below the bubble point, the single-phase oil turns into a two-phase fluid with rather high amounts of liquid, indicated by the quality lines within the phase envelope around the separator condition. Therefore, black oil is also called low-shrinkage oil. [5, pp. 311-313]

As its name implies, volatile oil falls victim to higher shrinkage because of quality lines which lie closely together below the bubble point line and low-percentage iso-vols at separator condition, as depicted on the right in Figure 9. A less heavy and also smaller C₇₊ fraction than in black oil shifts the cricondentherm to the left and the cricondenbar a little bit upwards. The color of volatile oil, alias near-critical oil, varies from green and orange to brown but it undergoes the same phase changes as low-shrinkage oil. [5, p. 313]

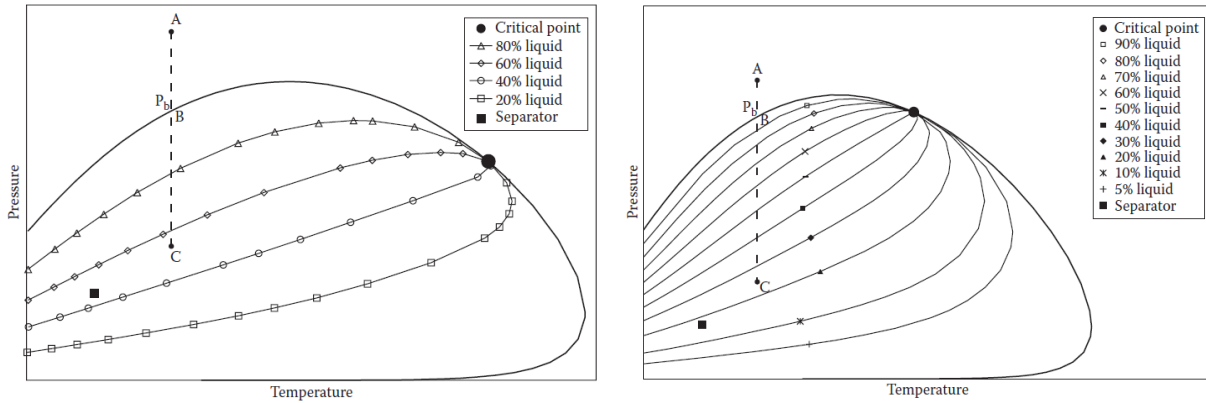


Figure 9: Typical Phase Diagram of Black Oil (left) [5, p. 312] and Volatile Oil (right) [5, p. 315]

Gas condensate experiences different phase changes because the initial condition is a single-phase vapor at a temperature between the critical temperature, which is lower than for volatile or black oil, and the cricondentherm and therefore crosses the retrograde dew point during a pressure decline. As already described in the case of a binary system in chapter 2.3.2.1, the first liquid droplets condense from the gas at the upper dew point. During further depletion, represented by the vertical dashed line in Figure 10, the lowest percentage iso-vol is crossed first, followed by higher ones until a maximum point, which is trapped by the same-valued quality line somewhere in the phase envelope. After this highest so-called liquid drop out, revaporization starts and the amount of liquid, which is usually not produced due to its immobility in the reservoir, decreases until the separator condition is reached. [5, pp. 315-318]

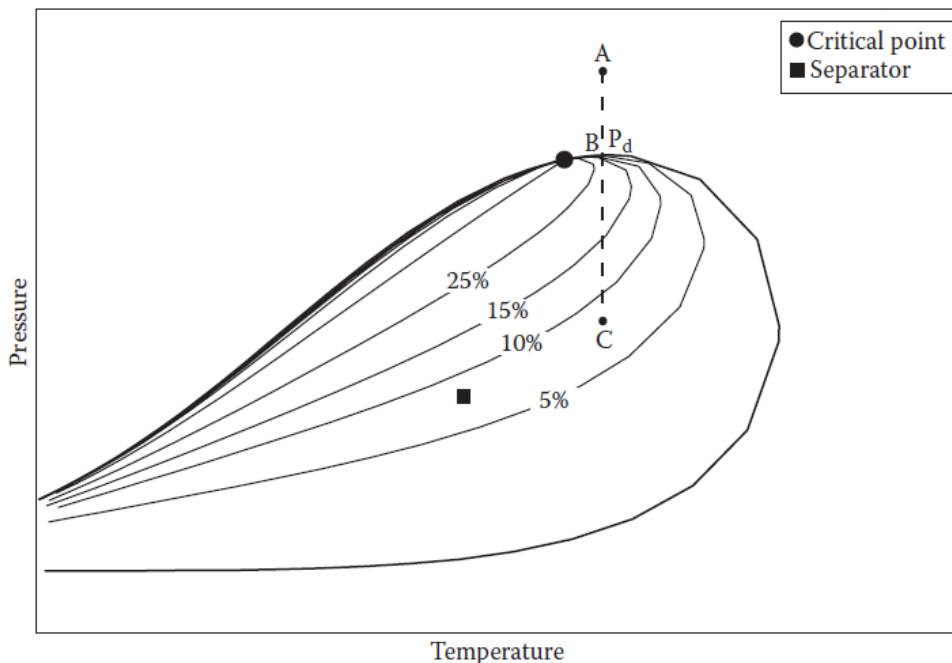


Figure 10: Typical Phase Diagram of Gas Condensate [5, p. 316]

Wet and dry gas are those reservoir fluids with temperatures higher than the cricondentherm of their respective phase envelope. Additionally, the two-phase area is much smaller compared to black oil, volatile oil and gas condensate. The terms wet and dry have nothing to do with presence or absence of water but rather with the position of the separator condition with respect to the phase envelope. On the one hand as seen in the left diagram in Figure 11, some liquid precipitates from the reservoir gas under separator conditions, and hence the name wet gas. On the other hand, the separator condition of dry gas, depicted on the right in Figure 11, is also in the single-phase area and therefore no liquid is formed at all. [5, pp. 318-319]

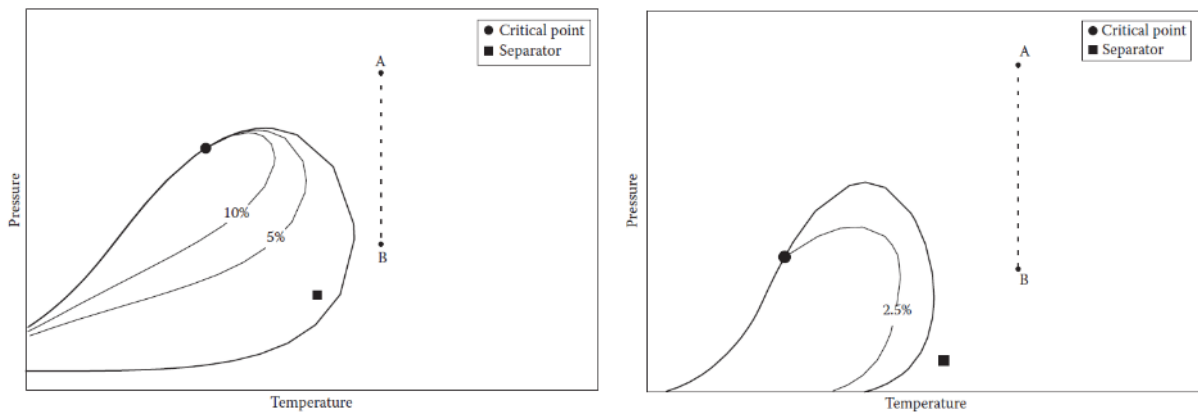


Figure 11: Typical Phase Diagram of Wet Gas (left) [5, p. 318] and Dry Gas (right) [5, p. 319]

For the sake of completeness and although the overall composition of the system stays the same for one particular phase diagram, it needs to be mentioned that the respective composition and chemistry of each phase during the equilibrium changes and varies with pressure and temperature. The trend though seems to be the same for binary and multicomponent systems as well as for different reservoir fluids. As an example, the mole fractions of methane and the C_{7+} fraction of a black oil system in equilibrium below the bubble point are shown in Figure 12. It seems to be obvious that lower pressures favor the evaporation of the lighter and volatile components and hence the relative amount of CH_4 in the liquid phase gets lower while the C_{7+} fraction increases. Contrary to this explanation, the methane fraction in the vapor phase does not merely raise. In fact, it just increases right below the bubble point while at lower pressures, also heavier components such as n-butane vaporize and therefore decrease the methane fraction in the vapor phase. The same applies to the C_{7+} fraction in the gaseous phase, which only gets lower right below the bubble point and then increases because of such low pressures that make evaporation of heavy components possible as well. [5, pp. 297-301]

As previously mentioned, this behavior is qualitatively the same in a dew point system, where the initial precipitation of n-butane is followed by a revaporization at lower pressures, which counteracts the expected trend of the vapor phase below the retrograde dew point.

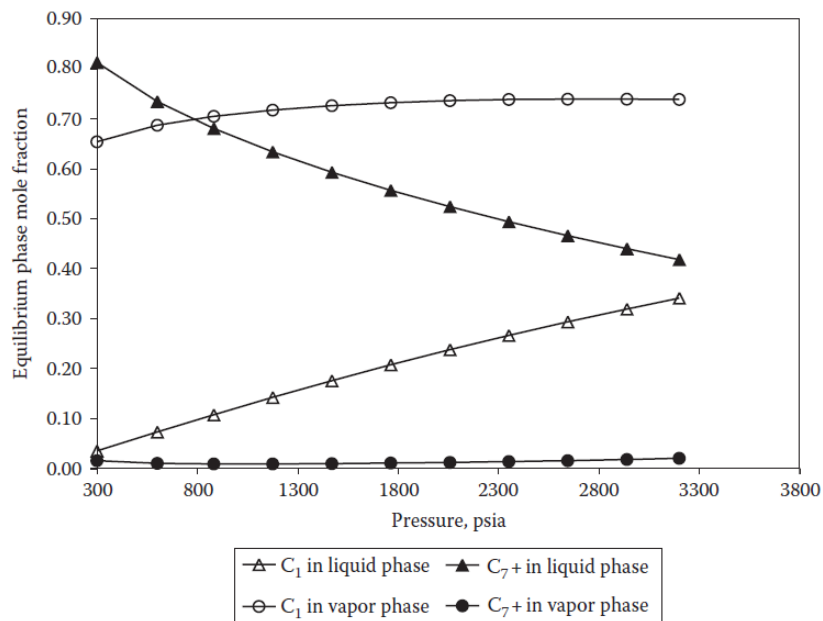


Figure 12: Behavior of the Phase Compositions in the Two-Phase Region of a Black Oil System [5, p. 320]

By measuring and plotting the phase densities as in Figure 13, decreasing pressure can be identified to be the dominant effect in the gaseous, while composition and the reduction of methane plays a more important role in the liquid phase. [5, p. 299]

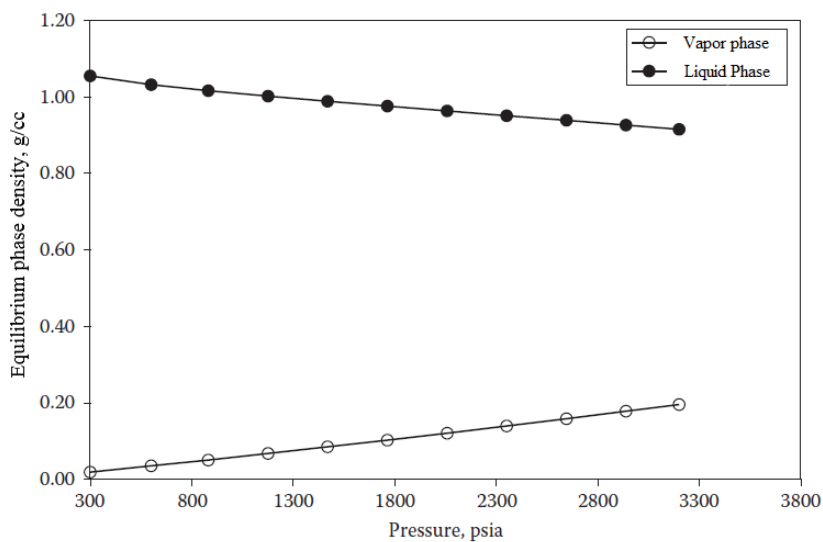


Figure 13: Phase Densities of a Black Oil System below the Bubble Point [5, p. 321]

2.3.3 Bubble Point and Dew Point Calculation

In order to construct a phase diagram of a specific reservoir fluid with a constant overall composition, it is crucial to determine bubble point and dew point pressures at various temperatures. These and the vapor pressure for a pure component, can either be determined by laboratory measurements or by means of prediction methods such as correlations and equations. Whereas the mathematical approaches are presented in this chapter, the laboratory measurements are introduced in chapter 2.3.4. It is worth mentioning that the phase envelope of dry gas can also be determined in the laboratory despite the fact that during production no phase changes occur. High costs and expenditure of time of laboratory measurements and lack of available samples are often aspects in mathematical approaches' favor, which are by the way not only restricted to the calculation of saturation pressures. These so called phase equilibrium or Vapor-Liquid Equilibrium (VLE) calculations usually need pressure, temperature, overall system composition and properties of all the individual components as input parameters. [5, pp. 439-440]

As a start, an ideal mixture without any molecule interaction is used to describe some basic principles, which can also be used for the determination of bubble and dew point of reservoir fluids. For this purpose, the two most important laws, namely the Raoult's and the Dalton's Law, are respectively mathematically shown in **eq.4** [5, p. 440] and **eq.5** [5, p. 441].

$$p_i = X_i * p_{vi} \quad (4)$$

p_i	partial pressure of component i in the gas phase [psia]
X_i	mole fraction of component i in the liquid phase [-]
p_{vi}	vapor pressure of component i at the given temperature [psia]

$$p_i = Y_i * p \quad (5)$$

Y_i	mole fraction of component i in the vapor phase [-]
p	total system pressure [psia]

By equating **eq.4** and **eq.5** as in **eq.6** [5, p. 441], and after rearranging, a new variable called equilibrium ratio, can be introduced as defined in **eq.7** [5, p. 441]. Because the vapor pressure refers to a pure component with a maximum number of degrees of freedom of two according to Table 5, the K factor calculated in this approach is only a function of pressure and temperature, irrespective of the overall composition of the hydrocarbon mixture. [5, p. 441]

$$X_i * p_{vi} = Y_i * p \quad (6)$$

$$\frac{p_{vi}}{p} = \frac{Y_i}{X_i} = K_i \quad (7)$$

To determine X_i and Y_i , which are the last two unknowns, additional equations need to be included. A material balance equation of a system with a specific overall composition, which is

flashed and moreover separated into a vapor and liquid phase at a certain pressure and temperature, is shown in **eq.8** [5, p. 442]. It states that the moles of component i in the feed must be the same as the sum of the moles of component i in the equilibrium liquid phase and the moles of component i in the equilibrium vapor phase.

$$Z_i * n = X_i * n_L + Y_i * n_V \quad (8)$$

Z_i	overall molar composition [-]
n	moles of the entire system on the feed [mol]
n_L	moles of liquid [mol]
n_V	moles of vapor [mol]

With the assumption of 1 mol of feed and by inserting **eq.7** into **eq.8**, the mole fraction of component i in the liquid phase can be expressed as **eq.9** [5, p. 443]

$$X_i = \frac{Z_i}{1+n_V*(K_i-1)} \quad (9)$$

or by including the conservation of mass as **eq.10** [5, p. 443].

$$\sum_{i=1}^n X_i = \sum_{i=1}^n \frac{Z_i}{1+n_V*(K_i-1)} = 1 \quad (10)$$

Analogue, **eq.11** [5, p. 443] applies to the mole fraction of component i in the vapor phase. Those two equations are often called the flash functions and are the basis of VLE calculations.

$$\sum_{i=1}^n Y_i = \sum_{i=1}^n \frac{Z_i * K_i}{1+n_V*(K_i-1)} = 1 \quad (11)$$

At this point, a starting value between 0 and 1 can be chosen for the remaining unknown n_V and iterated until the sum of the mole fractions equals 1. [5, p. 443]

Since n_V and n_L respectively converge towards 0 and 1 at the system pressure equal to the bubble point, the bubble point pressure can be calculated by inserting **eq.7** into **eq.11** as in **eq.12** [5, p. 444].

$$p_b = \sum_{i=1}^n Z_i * p_{vi} \quad (12)$$

Similarly, the dew point, where n_V and n_L respectively converge towards 1 and 0, can be calculated with **eq.13** [5, p. 445].

$$p_d = \frac{1}{\sum_{i=1}^n \frac{Z_i}{p_{vi}}} \quad (13)$$

However, the problem with this equation and approach is that pure components have no vapor pressure at temperatures above the critical point as shown in Figure 6 before. This limits the application for ideal mixtures to temperatures below the critical temperature of the lightest and most volatile component in the entire system. On the basis of CH₄ alone, it cannot be applied for many reservoir fluids because methane has a critical temperature of about -116°F or -82°C, which is not realistic for any practical condition at all. [5, pp. 445-446]

In some empirical correlations though, the equilibrium constant is calculated differently to overcome this restriction as shown in **eq.14** [5, p. 447], the Wilson Equation, where the K factor is a function of pressure, temperature and composition of the hydrocarbon mixture. It is worth mentioning that the acentric factor in the equation accounts for the deviation of the molecules from ideal sphericity.

$$K_i = \frac{p_{ci}}{p} e^{(5.37*(1+\omega_i)*\left(1-\frac{T_{ci}}{T}\right))} \quad (14)$$

K _i	equilibrium ratio of component i [-]
p _{ci}	critical pressure of component i [psia]
p	system pressure [psia]
ω _i	acentric factor of component i [-]
T _{ci}	critical temperature of component i [°F]
T	system temperature [°F]

A few other K factor calculation methods are based upon the of the convergence pressure fundament. This concept basically utilizes the fact that at a fixed temperature, plotted K_i factors of a system in equilibrium converge towards 1 at a specific pressure, called convergence pressure p_κ. According to **eq.7**, this is the result of X_i = Y_i, which is actually only the case at the critical point. Therefore, convergence is physically only possible at a fixed temperature equal to the critical temperature and hence this corresponding pressure, which is then also the critical pressure as well as the bubble point at this temperature, is called the true convergence pressure. [5, pp. 447-451]

As shown in a K value chart as Figure 14, at temperatures lower than the critical temperature, convergence does not occur because the equilibrium ratio is only defined until the bubble point, that is in this case lower than the convergence pressure at this temperature. Extrapolation is needed until the so-called apparent or imaginary convergence pressure, which is actually already in the single-phase area. By means of the previously explained phase rule, it can be proven that for a binary system, the equilibrium ratio is only dependent on pressure and temperature, while for a multicomponent mixture, it is also a function of the overall system composition. [5, pp. 447-451]

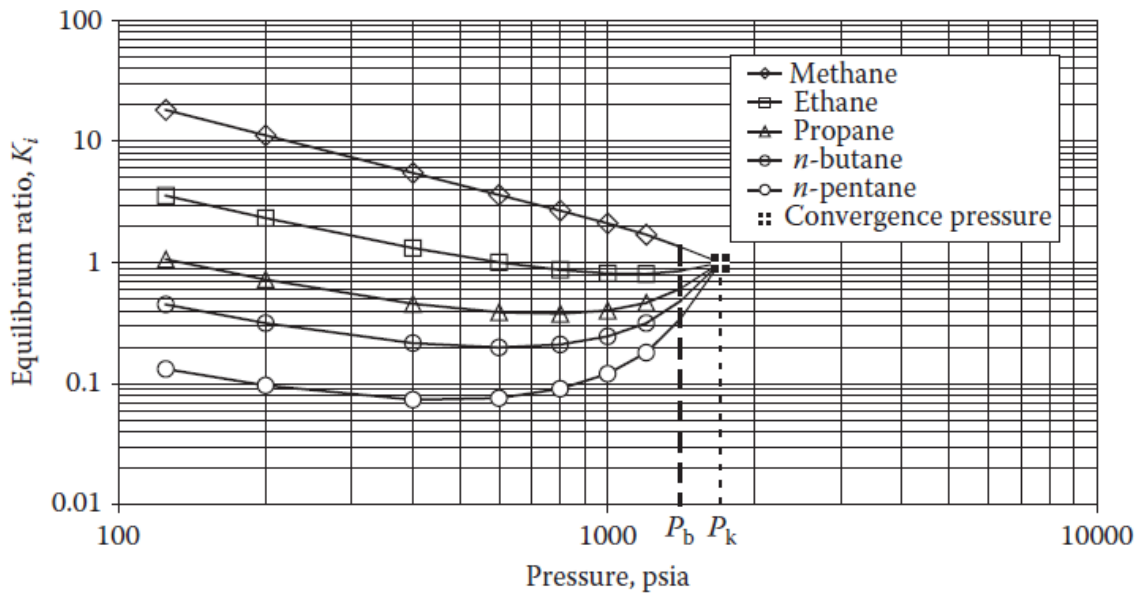


Figure 14: Equilibrium Ratios versus Pressure at a Temperature below the Critical One [5, p. 448]

With those K value charts, presented by the Natural Gas Processors Suppliers Association (NGPSA), and the knowledge that n_v converges towards 0 at the bubble point, equilibrium ratios for every component at different chosen pressures can be inserted into **eq.11** until the summation is correctly fulfilled and the bubble point pressure is found. It is important to mention that in the case of the bubble point calculation, the convergence pressure can directly be determined because of the knowledge of the liquid-phase composition, which equals the overall system composition of the feed in a bubble-point system. [5, pp. 453-454]

For the dew point determination though, where n_v converges towards 1, the liquid-phase composition is not known. Therefore, a convergence pressure needs to be assumed, followed by trial and error of equilibrium ratios at various pressures, and if needed, correcting of the previously assumed convergence pressure, until **eq.10** is satisfied. [5, p. 454]

Despite many available empirical and other equilibrium ratio correlations which can be applied in vapor-liquid equilibrium calculations, this approach is not very convenient. Equation-Of-State (EOS) Models as the well-known Soave-Redlich-Kwong equation, the Peng-Robinson equation and their extension for hydrocarbon mixtures, are beyond the scope of this thesis, even though they find more application in VLE calculations. [5, p. 457]

2.3.4 Laboratory Measurements

As repeatedly mentioned, chemistry, composition, pressure and temperature are the controlling parameters which define the state of a reservoir fluid. If fluid samples are available and costs and time of the experiments are worth performing them, measurements in so-called pressure volume temperature cells in laboratories are conducted to determine saturation pressures like bubble and dew point. These pressure vessels have a cylindrical shape, need to be capable of handling high pressures and temperatures and are therefore made of stainless steel or titanium with a small window out of sapphire for visual observations. The basic principle is the same for all different tests, namely, in- and decrease of pressure by changing the cell

volume usually at a constant temperature. During early days, this was achieved by injecting or draining mercury, which has been replaced by mechanical pistons nowadays. In some of these tests, emerging gas is removed, while the overall composition is retained in others. Additionally, the size of the cell depends on the compressibility of the reservoir fluid sample in a way that high compressible fluids need larger vessels than low compressible ones. What is also worth mentioning that the effect of water is ignored in all of these measurements, which is reasonable because of the lower gas solubility in water compared to oil. Figure 15 is a flow pattern, which shows the procedure of a typical PVT analysis with its possible outcomes like saturation pressures, liquid drop out and optimum separator conditions. After sampling either downhole or on surface, PVT experiments are conducted in cells suitable for the present fluid, as subsequently described. [5, pp. 397-399]

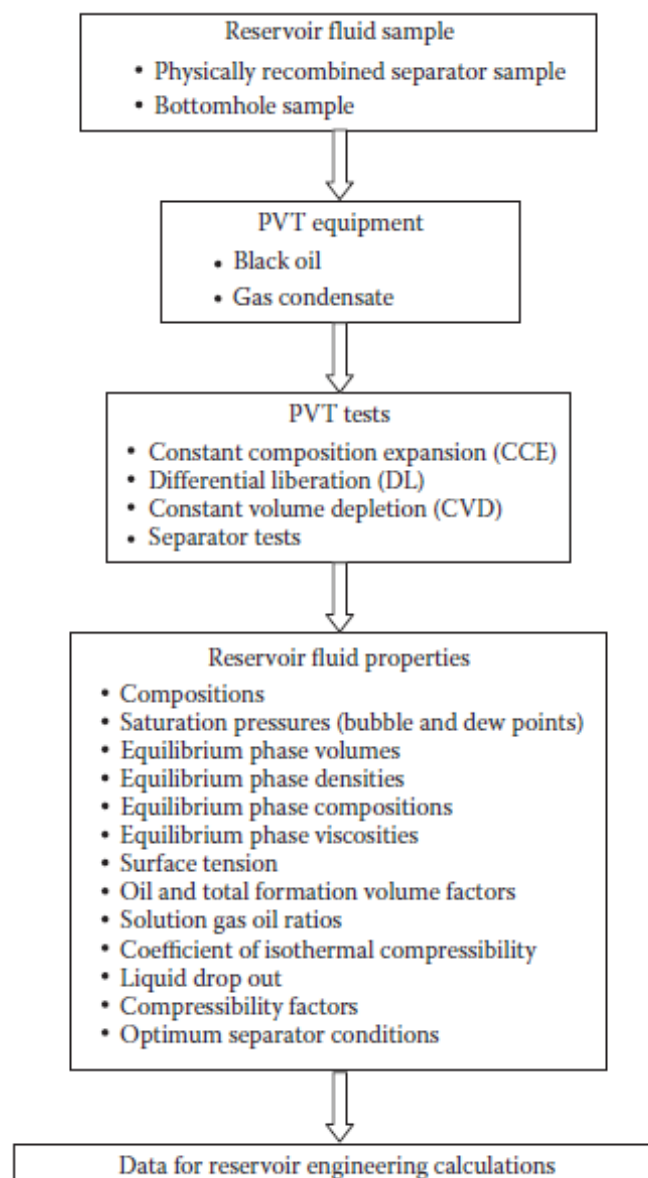


Figure 15: Flow Pattern of a PVT Analysis [5, p. 364]

One test, which can be executed with all kinds of reservoir fluids, is the constant composition expansion (CCE) experiment. The single-phase fluid is stabilized at reservoir pressure and temperature within the cell prior to the flash expansion due to volume increase at constant temperature as depicted for a gas condensate in Figure 16. Pressure is recorded and plotted versus total cell volume and depending on the fluid type, this can already be used for identification of the bubble point since a change in slope already indicates the liberation of compressible gas. However, for volatile oil, it is not as distinctive and obvious and hence the physical window in the cell should be used for visual evidence. To determine the entire bubble point and dew point curve, the tests need to be run at temperatures above the cricondentherm down to standard conditions. Especially for dry gas, it is necessary to perform the experiment at temperatures below the separator conditions, because during production, no phase change occurs. [5, pp. 399-401]

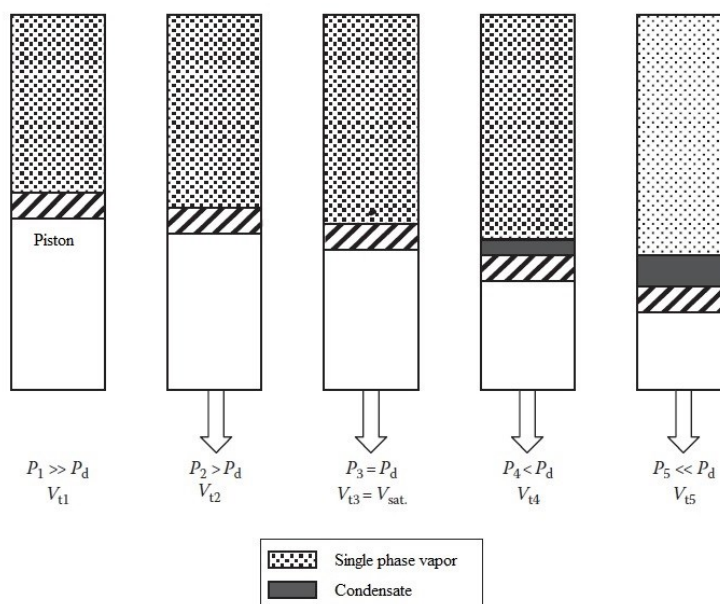


Figure 16: Constant Composition Expansion Test of a Gas Condensate [5, p. 400]

Reservoir oils are usually analyzed with a differential liberation (DL) test, which again starts above the saturation pressure at constant reservoir temperature. In this experiment, the pressure is then isothermally reduced below p_b and stabilized. During this first stage, the bubble point can be again determined visually through the cell window. The liberated gas is then isobarically removed by means of volume reduction as shown in Figure 17 and obviously leads to a change in overall composition of the sample during this test. Standard conditions are typically reached after 10 to 15 stages of pressure reduction and following gas withdrawal, which helps to determine properties like Z factor, formation volume factors, solution gas oil ratio, etc., and indicate in this context the so-called residual oil saturation. [5, pp. 401-402]

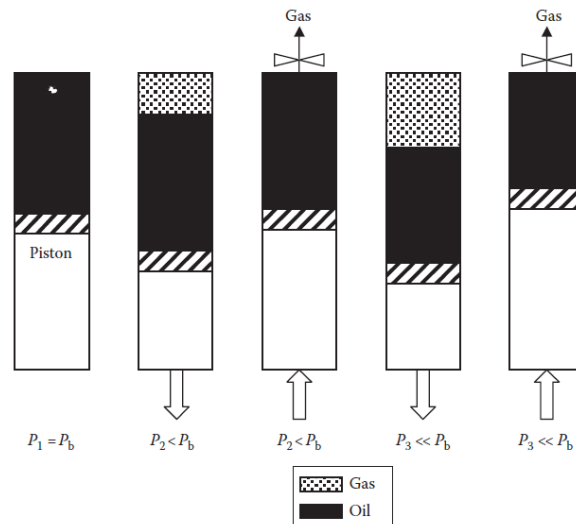


Figure 17: Differential Liberation Test of an Oil [5, p. 402]

Gas condensates are often analyzed with a constant volume depletion (CVD) test as shown in Figure 18. Again, the pressure is stabilized at constant temperature above the saturation pressure; in this case above the retrograde dew point, and then reduced until the first liquid drops out, indicating the saturation pressure and the so-called reference or saturation volume. Unlike in the case of a DL experiment, only as much gas is removed after every stage to regain the previously determined reference volume. This approach should simulate the constant pore volume in the case of a hydrocarbon reservoir with no water influx and the fact that the condensed liquid is not produced. In addition to the previously mentioned reservoir fluid properties, the liquid drop out curve can be determined during the CCE and CVD experiments. However, the values gained by the constant composition expansion test are usually higher because during the constant volume depletion test, gas that could condensate is already removed during earlier stages. [5, pp. 404-406]

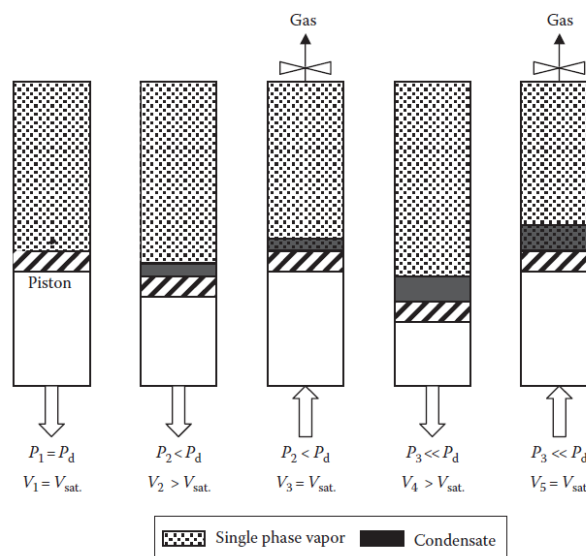


Figure 18: Constant Volume Depletion Test of a Gas Condensate [5, p. 405]

3 Separators

As already mentioned, the general usage and task of a separator is to split up a mixed inflow into its various phases, which are then emitted with a specific degree of purity through their respective outlets. The physical theory, the principle and the mathematics behind the phase separation processes are explained in this chapter. In addition, the unit and its components, as well as the several types and different configurations for variable operation areas and applications are presented.

3.1 Definition

In the oil and gas industry, a separator is usually referred to as the first vessel on surface, reached by the mixed well stream, in which phase separation starts. Most of the times, one separator alone is very inefficient and therefore not enough to achieve sufficient breakup. A gas oil separation plant (GOSP) though, which comprises more separators in varying configurations for several applications at different operation pressures for stage separation and other facilities like heaters, compressors, dehydrators, desalters, gas sweetening units, etc., exactly meets the requirements of a final and sufficient phase separation. The outflow of a previous stage then simply serves as the inflow of the subsequent stage, where the fluid is further processed until the various phases are sufficiently separated and what is more important: stable. [8, p. 71]

3.2 Types

Almost every reservoir fluid is different around the world and so are most of the separators. Therefore, many classifications have been introduced and one is shown in Table 7 to get a general idea of the supply and various types on the market.

Table 7: Classification of Separators

Number of Phases	Vessel Configuration	Application	Operating Condition
<ul style="list-style-type: none"> • Two-Phase • Three-Phase • (Four-Phase) 	<ul style="list-style-type: none"> • Cylindrical <ul style="list-style-type: none"> • Horizontal <ul style="list-style-type: none"> • Single Barrel • Double Barrel • Boot • Vertical • Spherical • Others <ul style="list-style-type: none"> • Centrifugal or Cyclone • Venturi 	<ul style="list-style-type: none"> • Production • Test • Scrubber • Filter • Slug Catcher • Free-Water Knockout 	<ul style="list-style-type: none"> • Low Pressure • Medium Pressure • High Pressure • Low Temperature

As in Table 7 already shown, separators can be classified according to the number of phases in which a mixture is split up. On the one hand, in the petroleum business, a two-phase separator removes either gas from oil and water for well streams from oil reservoirs, or gas from water if the produced mixture comes from gas reservoirs, in short, gas from the liquid. On the other hand, a three-phase vessel separates gas from the liquid, which is then additionally split up into water and oil. Solids, that are of course always present, are sometimes referred to as being the fourth phase, however, the expression four-phase separator is not commonly used. [8, p. 72]

Furthermore, it can be distinguished between cylindrical, spherical and some other differently shaped pressure vessels. Latter are for example centrifugal and Venturi separators, where an additional force is added to the system to support the separation. They are very rate-sensitive and the size of those configurations is limited and therefore, they are not used in oil and gas production because it definitely demands facilities capable of dealing with larger and sometimes intermittent quantities. Spherical separators are also rarely used because they are less efficient due to their short gravity settling zone, which is explained in detail in chapter 3.4.2 later on. Cylindrical separators, both vertical and horizontal as respectively shown in Figure 19 and 20, are most suitable for the separation during oil and gas production and hence they are examined within the rest of this thesis, with a focus on horizontal ones. [9, pp. 155-162]

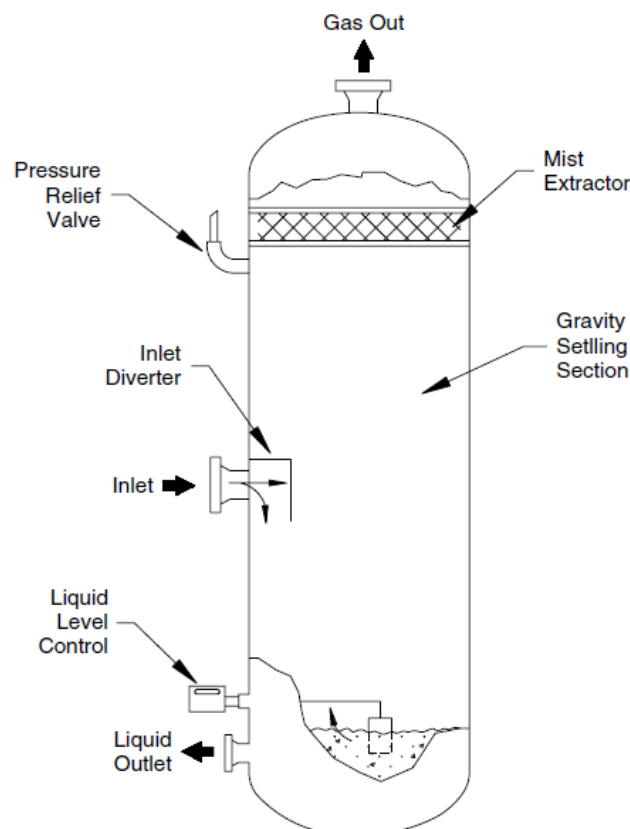


Figure 19: Cross Section of a Typical Vertical Two-Phase Separator [9, p. 157]

These two configurations do not really differ in their mode of operation; however, gas is separated more efficiently in horizontal separators due to the longer gravity settling section. Additionally, vertical separators cannot deal with larger slugs, which are introduced in chapter 3.4.3 later on.

In any case, the zones within a cylindrical separator, all the components, internals and their functionality are fully explained and described in chapter 3.4.

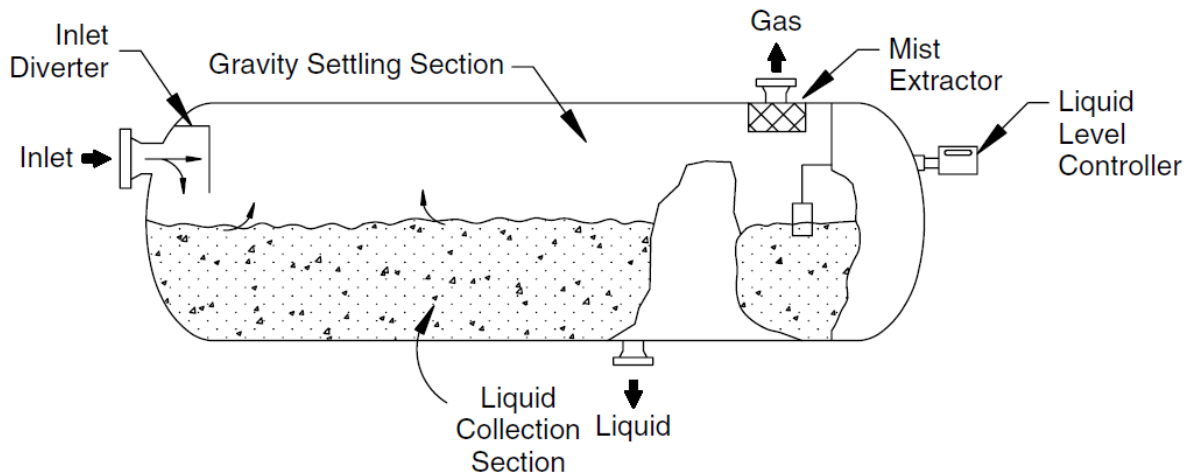


Figure 20: Cross Section of a Typical Horizontal Two-Phase Separator [9, p. 155]

Another classification of separators is based on their field of application and the most important examples are again shown in Table 7 before. As already mentioned, adequate separation is rarely achieved by a single production separator but a series of different facilities, thus a GOSP. A scrubber for example is a two-phase separator with the task of removing residual liquid from a gas phase during secondary separation. Therefore, it is usually installed after the gas outlet of a production separator and upstream of facilities, which cannot handle liquid, such as compressors, gas dehydration units, vent or flare outlets. So-called filters have similar applications, thus high GORs, and are also capable of removing tiny solid particles from the gas. The counterpart of those two types is the slug catcher, a two-phase separator that is able to deal with large slugs of liquid. It is applied at gas pipeline outlets after cleaning the tubes from accumulated liquid with a pig. The last mentioned example is the so-called free-water knockout, which removes the free water from the well stream and hence often represents the first stage during separation. The outcome of those vessels, which is then the inflow for further stages, is then less corrosive and the risk of emulsion and hydrate formation is lower. [9, pp. 163-165, 10]

The reason behind the application of separators at different operation pressures and temperatures, which are determined for example by means of a test separator, as shown in chapter 5.1, is based on the chemistry and composition and explained in chapter 3.3.

3.3 Phase Separation

As already mentioned, the mixed well stream, coming from one or more boreholes, needs to be separated into its various phases, namely one solid, two liquid and one gaseous. Water and solids do not change too much due to their low compressibility, however, gas and oil definitely alter, as accurately explained in chapter 2.3. Additionally, gas is not as prone to be dissolved in water as in oil. Phase separation of the dissolved gas and the oil during pressure reduction is crucial, while the already free gas just expands. Similar to the laboratory measurements in PVT cells, phase separation on a big scale can be initiated either continuously as in the case of a differential separation, or abrupt as a flash separation.

In general, a slower pace in pressure reduction, realized by multiple stages from high pressure to standard conditions, definitely leads to less liberation of gas and more stable oil and hence less shrinkage. The reason for that is based on the interactions and behavior during equilibrium of the different groups of components, namely light (C_1 & C_2), intermediate ($C_3 - C_6$) and heavy (C_{7+}) hydrocarbons. [8, pp. 75-77]

3.3.1 Differential Separation

On the one hand, pressure is lowered in stages during differential separation and the liberated gas is continuously removed, thus avoiding two-phase equilibrium of oil and gas. Therefore, only the lightest and some intermediate components are lost to the gas phase at every single stage, while most of the intermediate group and the entire heavy one remain in the oil. [8, pp. 76-77]

3.3.2 Flash Separation

On the other hand, pressure depletion is continued during flash separation even after establishment of a two-phase equilibrium. The preservation of the equilibrium postulates, that the gaseous phase gets heavier and heavier as the pressure sinks. At lower pressures, many intermediate and even heavy components are dragged along by the lighter components, resulting in a higher shrinkage of the oil. Since differential separation is very impractical and not feasible due to its many stages, flash separation is commonly applied, albeit a few stages are used to increase the oil recovery. [8, pp. 76-77]

3.3.3 Two-Phase - Gas and Liquid

Due to the diameter enlargement from the flow line to the separator, the velocity of the mixed stream decreases and the phases have time to separate in the lower pressure environment without much turbulences, which usually occur in the well or flow line. In a two-phase separator, gravitation separation is the only present process and hence the liquid settles down and the gas rises due to gravity, while a foamy interface forms in between. Latter is described in more detail later on in chapter 4.1.2.

The gravity settling of a liquid droplet in a different and continuous phase can be described, derived and predicted by setting up an equilibrium of forces acting on such a liquid droplet. The continuous phase can be either a gaseous and hence lighter one as in the case of two-phase separation, or another immiscible liquid phase, which can be lighter or heavier than the phase of the droplet, as explained in chapter 3.3.4. To start with, a force is defined, as known to all, as stated in **eq.15**.

$$F = m * a \quad (15)$$

F	force acting on the object [N]
m	mass of the object [kg]
a	acceleration of the object [m/s ²]

As shown in Figure 21, three forces usually act on the liquid droplet in the continuous gas phase within a two-phase separator, namely the gravity force F_g in **eq.16**, the buoyancy force F_b after Archimedes' Principle in **eq.17** and the friction or drag force F_d after Stokes' Law in **eq.18**. The gravitational force always acts down-, and buoyancy, as the name already says, upwards at all times, while the drag force is aligned with the movement of the friction-generating continuous phase.

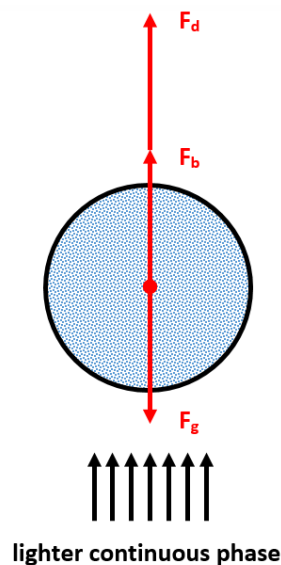


Figure 21: Force Equilibrium of a Heavier Phase in a Lighter Continuous Phase

$$F_g = m_{droplet} * g \quad (16)$$

F_g	gravity force acting on the liquid droplet [N]
$m_{droplet}$	mass of the liquid droplet [kg]
g	acceleration of the liquid droplet due to gravity [m/s ²]

$$F_b = m_{displaced} * g \quad (17)$$

F_b	buoyancy force acting on the liquid droplet [N]
$m_{displaced}$	mass of the volume which is displaced by the liquid droplet [kg]
g	acceleration of the liquid droplet due to gravity [m/s ²]

$$F_d = 3 * \pi * d * \mu * v_{settling} \quad (18)$$

F_d	drag force acting on the liquid droplet [N]
d	diameter of the liquid droplet [m]
μ	dynamic viscosity of the continuous phase [Pa*s]
$v_{settling}$	relative velocity or settling velocity of the liquid droplet [m/s]

By equalizing those equations as presented in **eq.19**, and after rearranging as shown below in **eq.20** and **eq.21**, the constant settling velocity, which is crucial for the sizing process of any separator, can be determined as shown in **eq.22**.

$$F_g = F_b + F_d \quad (19)$$

$$m_{droplet} * g = m_{displaced} * g + 3 * \pi * d * \mu * v_{settling} \quad (20)$$

$$\rho_l * V_{droplet} * g = \rho_g * V_{droplet} * g + 3 * \pi * d * \mu * v_{settling} \quad (21)$$

$$v_{settling} = \frac{(\rho_l - \rho_g) * V_{droplet} * g}{3 * \pi * d * \mu} = \frac{(\rho_l - \rho_g) * \frac{d^3 * \pi * g}{6}}{3 * \pi * d * \mu} = \frac{(\rho_l - \rho_g) * d^2 * g}{18 * \mu} \quad (22)$$

ρ_l	density of the heavier liquid droplet [kg/m ³]
ρ_g	density of the lighter continuous gas phase [kg/m ³]
$V_{droplet}$	volume of the liquid droplet [m ³]

However, **eq.18** in this form can only be applied for laminar flow or a lower Reynolds number, which is dimensionless and defined as stated in **eq.23** for fluid flow of spherical droplets in a continuous phase. Therefore, it needs to be rewritten in a form that can be corrected for possible turbulent flow by means of the drag coefficient C_D , which is equal to $24/Re$ for laminar flow, as shown and proven in **eq.24**.

$$Re = \frac{\rho_g * v_{settling} * d}{\mu} \quad (23)$$

$$\begin{aligned}
 F_d &= 3 * \pi * d * \mu * v_{settling} = 3 * \pi * d * \mu * v_{settling} * \frac{\rho_g}{\rho_g} * \frac{v_{settling}}{v_{settling}} * \frac{d}{d} = 3 * \pi * d^2 * v_{settling}^2 * \\
 \rho_g * \frac{1}{Re} &= 3 * \pi * d^2 * v_{settling}^2 * \rho_g * \frac{1}{Re} * \frac{4}{4} = 12 * A * v_{settling}^2 * \rho_g * \frac{1}{Re} = 12 * A * v_{settling}^2 * \\
 \rho_g * \frac{1}{Re} * \frac{2}{2} &= A * v_{settling}^2 * \rho_g * \frac{24}{Re} * \frac{1}{2} = C_D * A * \rho_g * \frac{v_{settling}^2}{2} \quad (24)
 \end{aligned}$$

A cross-sectional area of the liquid droplet [m²]

C_D drag coefficient [-]

The drag coefficient can then be approximated and determined by dint of correlations or diagrams either directly or through iterations. For the sake of completeness, the associated formula for the settling velocity is then determined in **eq.26**, after inserting the newly derived drag force formula into the force equilibrium of **eq.19** as shown in **eq.25**.

$$\rho_l * V_{droplet} * g = \rho_g * V_{droplet} * g + C_D * A * \rho_g * \frac{v_{settling}^2}{2} \quad (25)$$

$$v_{settling} = \sqrt{\frac{2 * (\rho_l - \rho_g) * V_{droplet} * g}{C_D * A * \rho_g}} = \sqrt{\frac{2 * (\rho_l - \rho_g) * \frac{d^3 * \pi}{6} * g}{C_D * \frac{d^2 * \pi}{4} * \rho_g}} = \sqrt{\frac{4 * d * g * (\rho_l - \rho_g)}{3 * C_D * \rho_g}} \quad (26)$$

3.3.4 Three-Phase - Gas, Oil and Water

Additionally to the separation of liquid and gas in a two-phase environment, which can be described by the same formula as in chapter 3.3.3, the different liquid phases split up in a three-phase separator according to their densities with an emulsion in between. During this process, free water is defined as the portion, which separates due to gravity settling. However, there is some part of the water, namely emulsified water, which cannot be separated by means of gravitation. A water in oil emulsion or with increasing water cut, an oil in water emulsion, must be separated either by dint of heat, chemical or electrostatic treatment. These methods and the issue of the formation of foam between the gaseous and liquid phase are examined in chapter 4.1.

In a three-phase environment it can happen that the liquid droplet is surrounded either by a lighter phase, as in the case of a water droplet in a continuous oil phase, or heavier, as in the event of an oil droplet in the circumjacent water phase. The former results in a settling velocity formula, shown in **eq.27**, similar to the previous derived equation due to the same force equilibrium as depicted in Figure 21 before.

$$v_{settling} = \sqrt{\frac{2 * (\rho_w - \rho_o) * V_{droplet} * g}{C_D * A * \rho_o}} = \sqrt{\frac{2 * (\rho_w - \rho_o) * \frac{d^3 * \pi}{6} * g}{C_D * \frac{d^2 * \pi}{4} * \rho_o}} = \sqrt{\frac{4 * d * g * (\rho_w - \rho_o)}{3 * C_D * \rho_o}} \quad (27)$$

ρ_w density of the heavier water droplet [kg/m³]

ρ_o density of the lighter continuous oil phase [kg/m³]

However, as highlighted in Figure 22, latter involves a different approach as in **eq.28** and **eq.29**. This then leads to a settling velocity, which is dominated and characterized by the buoyancy force and shown in **eq.30** with a different arrangement of the densities than in the previous cases, despite of the support of the drag force in direction of the gravitation. Because of that, it is more appropriate to call it rising velocity, or just terminal velocity, which can be used at all times for both directions.

$$F_g + F_d = F_b \quad (28)$$

$$\rho_o * V_{droplet} * g + C_D * A * \rho_w * \frac{v_{rising}^2}{2} = \rho_w * V_{droplet} * g \quad (29)$$

$$v_{rising} = \sqrt{\frac{2 * (\rho_w - \rho_o) * V_{droplet} * g}{C_D * A * \rho_w}} = \sqrt{\frac{2 * (\rho_w - \rho_o) * \frac{d^3 * \pi}{6} * g}{C_D * \frac{d^2 * \pi}{4} * \rho_w}} = \sqrt{\frac{4 * d * g * (\rho_w - \rho_o)}{3 * C_D * \rho_w}} \quad (30)$$

heavier continuous phase

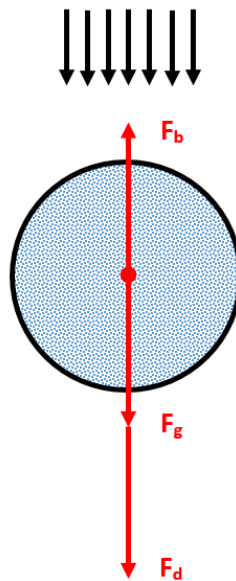


Figure 22: Force Equilibrium of a Lighter Phase in a Heavier Continuous Phase

3.4 Set-Up

The inner life of all separators, including those presented in chapter 3.2, can basically be subdivided into four functional sections as highlighted in Figure 23. Those are called the inlet section (brown), the gravity settling section (green), the liquid collection section (blue) and the mist extraction section (red) and are explained in this chapter. Additionally, all the internals and components are described in the following. [9, p. 154]

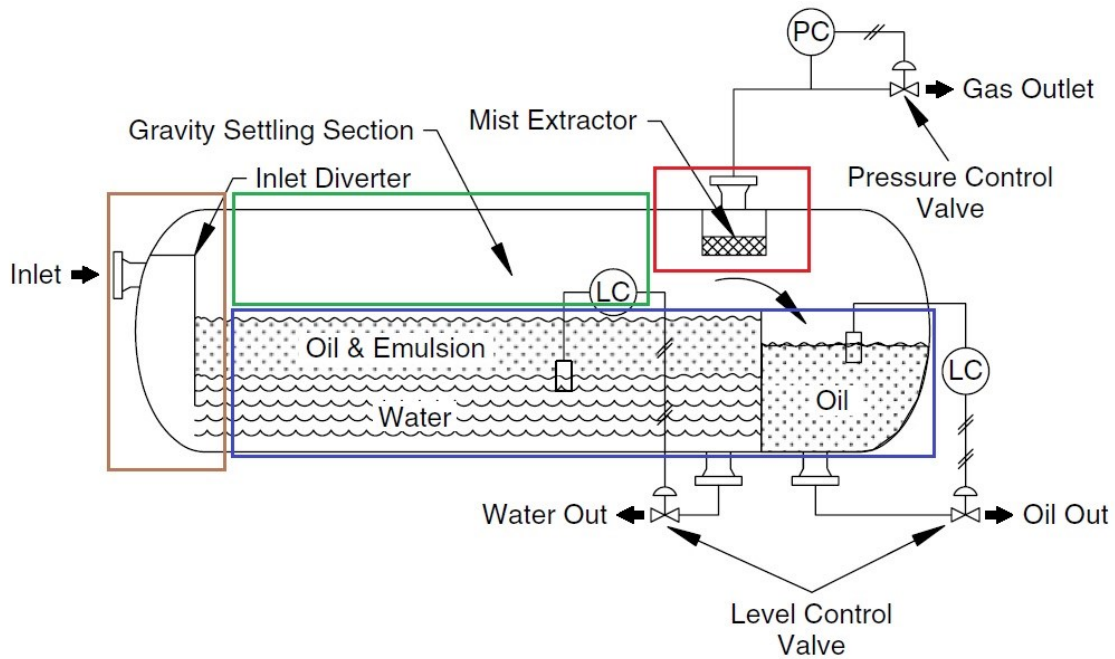


Figure 23: Cross Section of a Typical Horizontal Three-Phase Separator [9, p. 246]

3.4.1 Inlet Section

In the first section of a separator, the mixed well stream enters the vessel and immediately hits the inlet diverter, which leads to an abrupt change in direction and velocity. This internal can be either baffle plate diverter, as shown in Figure 24, or a centrifugal diverter. Latter is very rate-sensitive, much more expensive and for these reasons not as popular. The primary gross separation of gas from the liquid and solids in this zone is the result of the lower kinetic energy of gas at the same velocity due to its lower density, and hence the higher ability to change direction and stream around the diverter. [9, p. 154]

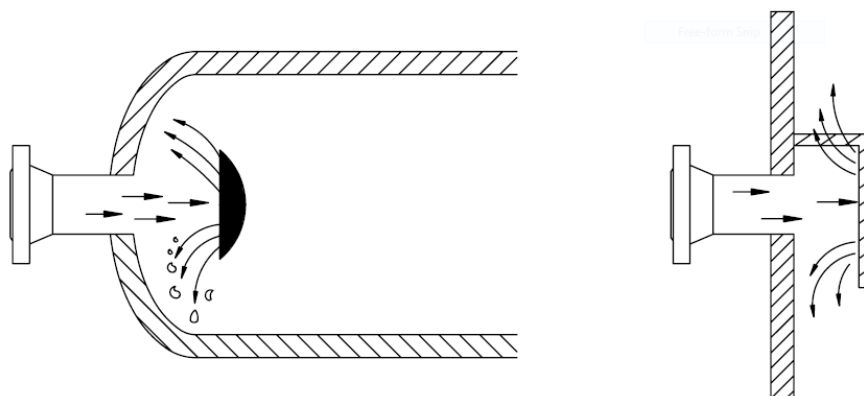


Figure 24: Baffle Plate Diverters - Spherical Dish (left) and Flat Plate (right) [9, p. 169]

While the gas migrates further into the separator, the liquid is ideally redirected by an inlet diverter to the bottom of the vessel as shown in Figure 25. This so-called Down Comer prevents the liquid from hitting the surface of the oil in the liquid collection zone, which would not only disturb the liquid level control, but would also lead to another mixture of the already

separated oil and water. Further, the water droplets immediately encounter the free water, coalesce and hence oil-water separation is promoted. Therefore, this is often also called water washing. [9, pp. 246-247]

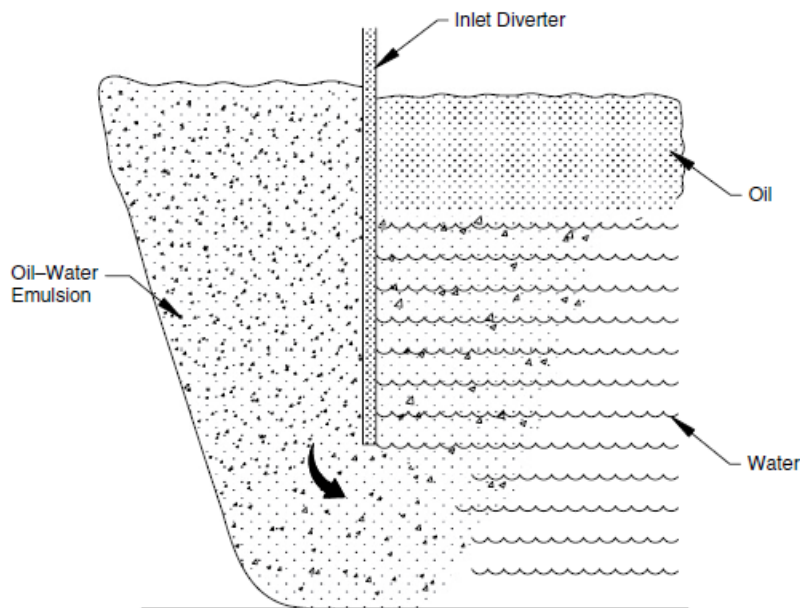


Figure 25: Down Corner Inlet Diverter [9, p. 247]

3.4.2 Gravity Settling Section

The processes in the gravity settling section go on according to the phase separation described in chapter 3.3.3.1. Water and oil settle down while the gas and some smaller liquid droplets continue to stream in horizontal direction towards the so-called mist extractor. Absence of turbulences due to the larger diameter compared to the tubing in the well or the flow line favors the phase separation. The already mentioned formation of foam, which is examined in chapter 4.1.2, occurs exactly between the gravity settling section and the underlying zone, which is described in the next paragraph. Defoaming plates, as shown in Figure 26, are slanted parallel steel sheets, which provide much surface for foam bubbles to collapse. [9, p. 173]

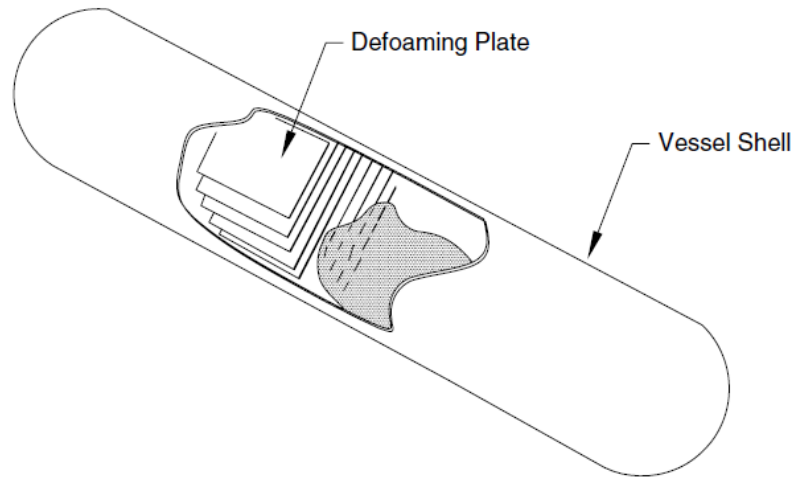


Figure 26: Defoaming Plates [9, p. 173]

3.4.3 Liquid Collection Section

In the liquid collection section, the fluids again separate according to their densities, with an oil pad on top, oil in water or water in oil emulsions in between, and the free water at the bottom. The time which takes the liquids to move from one to the other end of the separator has to be adequate to not only allow the liquid separation, but also to establish an equilibrium between the gaseous and liquid phases at the operating pressure and hence to allow the residual gas to come out of solution. This so-called retention time plays an important role in the design process of a separator and is therefore explained in chapter 5.2. later on. Further, an interface level controller between the oil and water steers the water outlet on bottom in such a way that the oil-water interface is always at the desired height and only water is discharged. The oil on top can then flow over a weir, which separates the zone with water and oil from the zone with only oil, and out of the oil dump valve. Latter is steered by a liquid level controller to prevent any gas to be discharged together with the oil. [9, pp. 247-248]

Despite the inlet diverter after the separator inlet, big liquid surges can cause wavy motion in the liquid collection section, which can lead to undesired liquids slopping over the weir into the pure oil zone. Further, the interface level controller is disturbed by the alternating gas-liquid interface due to waves. So-called wave breakers are just vertically arranged perforated semicircular plates, which damp this unwanted movement. [9, p. 170]

Another important component in most of the separators is the vortex breaker, an element installed right in front of the water and liquid outlet. It usually has radial vanes in order to stop any angular motion and hence prevent the formation of vortices or whirlpools during the drainage of the respective liquid, which would lead to an unregulated outflow. While a swirl at the oil outlet would result in gas sucked out together with the liquid, emulsions could be drained together with the water through its outlet. [9, p. 173]

The last key components in the liquid collection section worth mentioning are the sand jets and drains, presented in Figure 27. As already mentioned, the stream coming from the well is often a mixture of gas, oil, water and fines. Due to the highest density of all the present phases, these solid particles usually settle down at the bottom of the separator, accumulate and subsequently reduce the volume of the separator and hence its efficiency. Therefore, produced water is injected through the nozzles and the fines are flushed out through the drains. [9, p. 175]

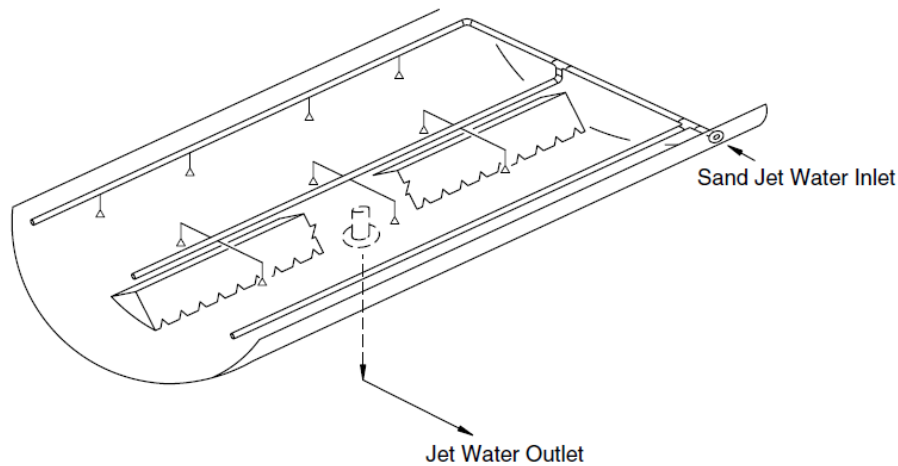


Figure 27: Sand Jets and Drains [9, p. 175]

3.4.4 Mist Extraction Section

On top of the separator and prior to the gas outlet, a mist extractor is installed to remove the small liquid droplets from the gas, which did not settle down in the gravity settling section. Capture of liquid droplets in a mist extractor obeys three different mechanisms, shown in Figure 28. Normally, gas streams around an obstacle as indicated by the arrows in Figure 28. However, droplets bigger than 1 micrometer are forced to keep moving straight due to inertia and consequently crash into the obstruction, which is in this case just a part of the mist extractor. The second mechanism is dominant for droplets or particles between 0.3 and 1 micrometer and therefore light enough to follow the gas streamlines. Nevertheless, if those flow lines are so close that the liquid droplets get in contact with the obstacle, they are captured on the surface. Random Brownian motion of droplets smaller than 0.3 micrometer due to collision with the gas molecules towards the obstacle is the last mechanism present in a mist extractor during particle capture. [9, pp. 176-178]

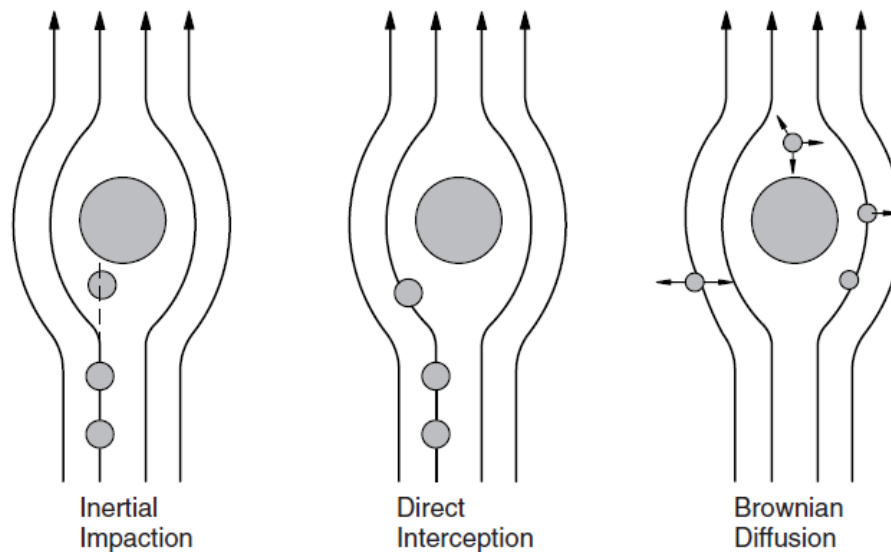


Figure 28: Liquid Droplet Capture Mechanisms in a Mist Extractor [9, p. 177]

Generally, it can be distinguished between an impingement and a centrifugal mist extractor type. On the one hand, latter is very rate dependent and expensive, similar to the centrifugal inlet diverter. Therefore, it is not very common, except for situations where plugging is an issue. On the other hand, there are several versions of impingement type mist extractors, namely the wire-mesh, the baffle and the micro-fiber, which are compared in Table 8. The most common and cheap wire-mesh mist extractor is composed of either woven or knitted stainless steel wires and has the form of a cylinder with enough void volume for the fluid flow and reasonable gas and liquid capacities. Droplet sizes of 3 to 10 micrometers and above are almost completely removed because they impinge on the wires' surface, accumulate and coalesce until they reach a sufficient weight to fall down into the liquid collection section. The pressure drop along this mist extractor is not that much, however, it is important to operate at an adequate pace. A too low gas velocity would allow the liquid droplets to follow the streamlines around the wires while already sinking liquid would be recaptured and carried along with the gas towards the gas outlet. Furthermore, it is not the best option if solids are present because this version is prone to plugging. [9, pp. 177-187]

Table 8: Characteristics and Comparison of Impingement Type Mist Extractors [9, p. 188]

Consideration	Wire-Mesh	Vane	Micro-fiber
Cost	Lowest	2–3 times wire-mesh unit	Highest
Efficiency	100% (for droplets larger than 3–10 μ)	100% (for mists > 20–40 μ)	Up to 99.9% (for mists < 3 μ)
Pressure drop	< 25 mm H ₂ O	< 15 mm H ₂ O	100–300 mm
Gas capacity	Very good	Up to twice that of a wire-mesh unit	Lowest
Liquid capacity	Good	Best	Lowest
Solids	Good	Best	Soluble particles with sprays only

The second impingement type is called the vane or baffle mist extractor and it basically consists of a series of parallel plates which must not provide a straight flow path, but one with a spacing wide enough to avoid turbulences. The separation principle is based on the change in direction of the gas stream flow, resulting in inertia impaction of droplet sizes between 20 to 40 micrometers, followed by a backflow down into the vessel. Due to the spacing of the plates, the pressure drop is lower, the fluid capacities are higher and it is less susceptible to plugging compared to the wire-mesh mist extractor. Very fine droplets or to be more precise, smaller than 3 micrometers, can only be removed by means of the last presented impingement type mist extractor, called the micro-fiber. It has a similar setup as the mesh-wire version but much finer wires, thus micro-fibers. Since this element is very tightly packed, liquid droplets smaller than 3 micrometers can be removed from the gas stream. Due to this tightness, the pressure drop is fairly high and fluid capacities are rather low. [9, pp. 178-187]

The sizing of mist extractors should be done by the manufacturers since the stated pressure drops significantly vary among all the providers. In addition to the mist extractor in the mist extractor section, a gas backpressure valve is built-in to maintain constant operating pressure of the separator. [9, p. 190]

4 Separator Performance

As every tool, device or machine, a separator type is selected, equipped with necessary internals and designed for specific operating conditions and criteria to achieve the optimum efficiency. If some unpredictable or unexpected incidents disturb the separation process, the performance gets worse or the entire breakup even ineffective. The internals and components, which have been described in chapter 3.4, usually enhance the separation process but exactly those are often the weakest point of the pressure vessel and hence prone to failure.

4.1 Issues

All the problems and issues in a separator, the reasons for their occurrence and how to prevent or at least counteract them are examined in this chapter. Included are those normally solved by the internals as sloshing, foaming, liquid carry-over, gas carry-under and emulsions and those, which affect exactly these components, as paraffin or corrosion. Sand and salts, which have been already broached in chapter 3.4.3 before, affect the installations in a separator, but are also solved by them as shown in this chapter.

4.1.1 Sloshing and Slugs

Sloshing is referred to as liquid motion within an object and therefore it is more likely to occur in separators, which are installed offshore. However, those wavy actions inside the pressure vessel can also be the result of the already mentioned slugs, in other words, intermittent inflow into the separator. Especially in parts with lower elevation along the flow line upstream the vessel, liquid can accumulate to a point where there is no remaining portion of the cross-section for the gas to bypass. The pressure builds up until the liquid is abruptly pushed further, directly into the separator. The previously explained inlet diverters definitely diminish this problem, however, the weir has to have a safety margin at all times and the interface level control and the level control need to shut in in the worst case to avoid any undesired and unseparated outflow through the liquid outlet. [9, pp. 194-195, 11]

4.1.2 Foaming

As already mentioned several times, a well stream is not only a mixture of different phases, but also a mix of many different components and compounds, as listed in chapter 2 during the characteristics of crude petroleum. Undesired impurities as natural CO₂ and constituents of fluids, introduced by the human being during drilling, completion, workover or injection, often result in the formation of foam at the gas-liquid interface in the separator. Compatibility should of course always be checked before any intervention or action during laboratory tests because error prevention is better than correction at all times, however and unfortunately, the human is still the biggest malfunction source. The problems which come along with foam are the high volumes, which decrease the designed liquid and gas capacities, see chapter 5.2, and hence the separator's efficiency. Additionally, the interface level controller is disturbed and foam could exit the gas or liquid outlet, which is then respectively called, gas carry-under and liquid carry-over. The already mentioned defoaming plates definitely eliminate occurring foam to a certain

extent but if that does not help anymore, chemicals, called depressants, need to be added. Again, compatibility has to be checked before and also the fact, that it alters the hydrocarbons, should be considered. [8, pp. 90-91, 9, pp. 190-191]

4.1.3 Liquid Carry-Over

Liquid leaving the separator through the gas outlet is called liquid carry-over and it can be related to foaming as previously explained. Additionally, it is of course also possible that the separator has been undersized with regards to the liquid capacity or the reason behind is simply a plugged water outlet or a too high inlet flow rate. In any case, the interface level controller and liquid level controller need to shut in the inlet of the separator. A level safety high (LSH) sensor usually detects a too high liquid level and the controller then stops the influx. [9, pp. 192-193]

4.1.4 Gas Carry-Under

The equivalent incident at the water or oil outlet is called gas carry-under or gas blow by and it is the undesired gas outflow together with the liquids. One cause can be the already mentioned vortexing, where gas could be sucked out by an occurring whirlpool. However, this can usually be prevented by a vortex breaker, introduced in chapter 3.4.3. A too low liquid level due to under sizing of the separator's gas capacity can also be a reason for gas carry-under, but should be detected by a level safety low (LSL) sensor in an interface or liquid level controller. Latter then shuts in either the liquid outlets only or both, the liquid outlets and the inlet of the separator. In any case, subsequent pressure vessels should definitely be equipped with a pressure safety valve to release some pressure in the event of a gas blow by. [9, pp. 193-194, 11]

4.1.5 Wax

At temperatures below the so-called cloud point, which depend on the crude oil composition, heavy paraffins or wax, can start to form and clog internals such as the defoaming plates or the wire-mesh and micro-fiber mist extractors. As already mentioned, the centrifugal type or the vane mist extractor are not very prone to plugging and therefore the better choice for some crudes. Despite the effort to operate above the cloud point or wax appearance temperature, man ways, hand holes and nozzles can be integrated in a separator to remove the wax or to fight against its appearance. Steam, which increases the temperature of the system, or solvents, which need to be adapted to the present crude oil, can be injected to dilute that solid petroleum. [8, p. 90, 9, p. 192, 11]

4.1.6 Sand

SiO₂, also known as quartz and which is the main constituent of sand, has a hardness of 7 on the Mohs Hardness Scale and is very abrasive. Especially all the internals suffer erosion and wearing and therefore it is recommended to temper all the elements that are directly exposed to the impact of the sand particles such as the inlet diverter or defoaming plates. In addition to that, the wire-mesh and micro-fiber mist extractors are also very prone to be clogged, already

mentioned as in the case of wax appearance, and therefore not the ideal choice for very sandy crudes. However, due to its highest density compared to the fluids, the solids usually accumulate at the bottom of the separator, where nozzles and drains are built-in for removal. [8, pp. 91-92, 9, p. 192]

4.1.7 Corrosion

Since most internals of the separator and the pressure vessel itself are made of metals, or more specifically steel, corrosion is a day-to-day issue. Especially very salty fluids are highly corrosive and the presence of H₂S or CO₂ accelerate the oxidation even more. An internal plating or coating out of synthetic material definitely postpones corrosion and a highly active sacrificial or galvanic anode protects the less active metals of the pressure vessel by oxidizing itself. It is also recommended to oversize the wall thickness of all pressure vessels to allow for safe tightness over a longer period of time. Corrosive damage can be detected by nondestructive testing (NDT) as ultrasonic measurement surveys.

4.1.8 Emulsions

The already a few times mentioned emulsions are stable mixtures of two immiscible liquid phases with the internal phase being dispersed in the external or continuous phase. There are basically two different types, namely the more common water in oil emulsion and the oil in water emulsion during higher water cuts. In addition to the presence of two immiscible liquid phases, which is only the case in a three-phase separator, agitation responsible for the dispersion and an emulsifying agent for the stabilization need to be in place. Depending on the type and amount of the present impurities, an emulsion does either split up very slowly or never due to gravity alone. Those emulsifying agents have a hydrophilic head and a hydrophobic tail and form a kind of skin around the dispersed droplets. They can be either naturally present or even introduced by the human being during drilling, completion, workover or injection. Besides interfering with the interface level controller, the efficiency of the separator change for the worse if those emulsions are not broken. This can be achieved by means of heat, chemical or electrostatic treatment mostly prior to the production separator, as described in the following. After breaking the emulsion, gravity settling becomes effective since the smaller droplets are then able to coalesce. [8, pp. 153-156]

4.1.8.1 Heat Treatment

The first option to break an emulsion is the application of heat and the resulting temperature increase, however, this is not done within a separator but upstream in a so-called heater. In any case, a higher temperature leads to a lower oil viscosity, favoring the settling of the water droplets in the continuous oil phase. Unfortunately, a temperature increase also leads to a higher shrinkage of oil due a higher tendency of gas liberation and hence downgrades the quality of the oil. Additionally, fuel costs for the heating process should not be neglected. [8, pp. 162-164, 9, p. 403]

4.1.8.2 Chemical Treatment

Surface-active agents, similar to those stabilizing the emulsion, can be used to neutralize this effect and hence break the emulsion. The demulsification procedure can be structured into two sub-processes; the flocculation and the coalescence. During the former, the demulsifier or emulsion breaker creates an attraction between the dispersed water droplets and they congregate. Subsequent coalescence, also caused by the emulsion breaker, leads to droplets, which can then be separated due to gravity settling. The selection of the appropriate demulsifier, which by the way all work differently, and the correct amount is therefore a tightrope walk and depends on many factors as density difference, droplet diameter, viscosity, surface tension, salinity, age of the emulsion and agitation. [8, p. 169]

4.1.8.3 Electrostatic Treatment

The last method to break emulsions is based on a high-voltage electrostatic field and performed in discrete vessels, called electrostatic coalescers. In a water in oil emulsion, the dispersed conductive droplets are coalesced due to three emerging effects, which have something in common with each other, to wit additional droplet movement and hence an increased chance for collision and coalescence. Polarization forces the water droplets to orient towards the electrostatic field, which minimizes the distance between negative and positive poles and hence promotes attraction and coalescence. Further, water is pulled to the electrode and droplets gather and combine until they are heavy enough to settle down. At last, the electrostatic field degrades the skin, formed by the emulsifying agent. [8, pp. 172-173]

4.2 Efficiency Control

The efficiency control of a separator of course depends on the type and its application. A standard first stage production separator is usually rated and assessed based on two criteria. The former states that the gas stream leaving the gas outlet must not contain liquid droplets bigger than 10 micrometers, otherwise its performance is considered to be inefficient or simply bad. Since the droplet size distribution of an incoming well stream varies from case to case, it is crucial to analyze it during laboratory tests in order to also correctly define the droplet size to be removed during the separator sizing, which is explained in chapter 5. The second and last common criterion does not permit a liquid carry-over of more than 0.1 gal/MCF. Some other criteria for pipelines demand oil having less than 1% water and gas has to have less than 5 lbm water/MMscf. [8, pp. 116-118, 11]

5 Separator Sizing

In order to size the separator with respect to its dimensions, minimum and maximum flow rate, operating pressure and temperature, physical properties of the present media, the desired droplet diameter to be separated as well as the so-called retention times need to be known and specified. In any case, all those variables serve as important input parameters for the sizing procedure, where future changes should also be considered since a reservoir alters over time.

5.1 Operating Conditions

Laboratory measurements, as previously described in chapter 2.3.4, are crucial to identify the physical properties and operating pressure of oil and gas separators, regardless of whether one or more stages are needed. As already mentioned in chapter 2.3, the compositions of the phases change during pressure decline and separation and hence the optimum conditions need to be found in order to end up with the most valuable fluids. During separation tests, various different parameters are measured at different operating pressures and temperatures and compared afterward. Minimum oil formation volume factor, minimum gas oil ratio and maximum API gravity, are the governing criteria as shown by an example in Figure 29 and Figure 30. [5, pp. 412-413]

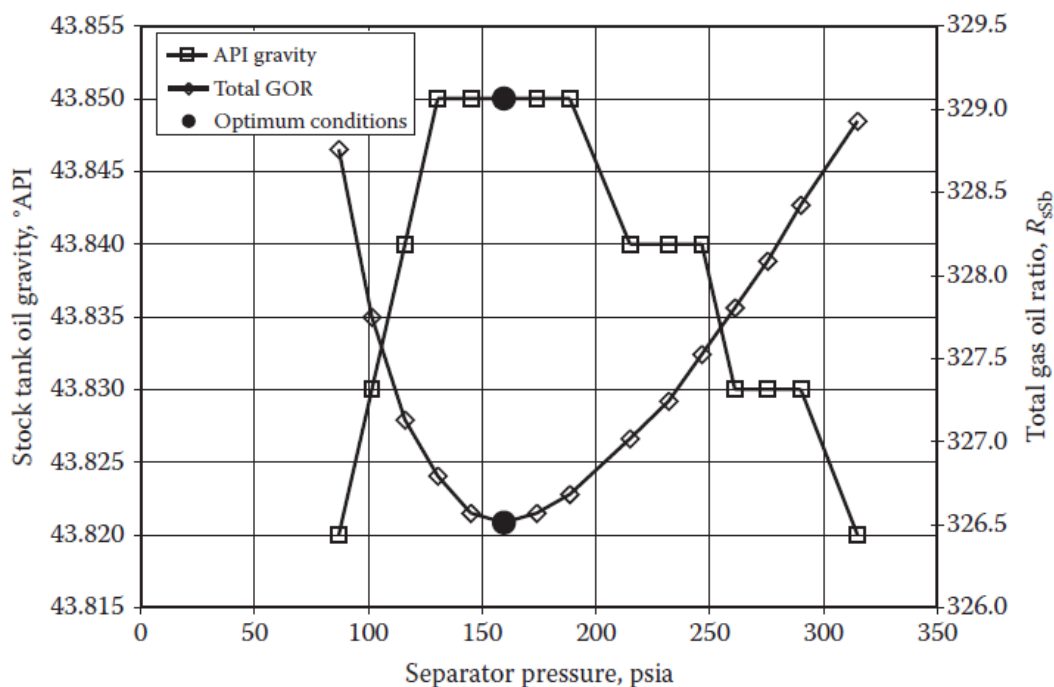


Figure 29: Determination of the Optimum Operating Conditions based on Oil Gravity and Gas Oil Ratio

[5, p. 414]

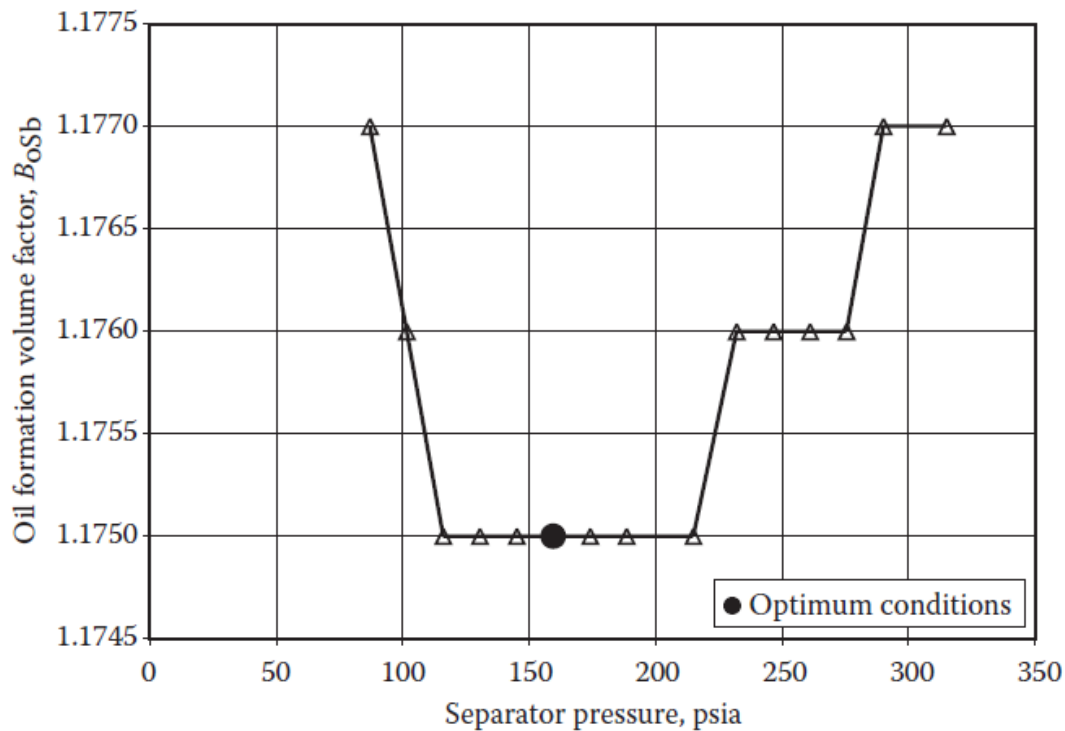


Figure 30: Determination of the Optimum Operating Conditions based on Oil Formation Volume Factor [5, p. 414]

By plotting these three parameters versus pressure, in this case at the already ideal constant separator temperature of 80°F, the optimum operating pressure of 159.5 psia is found. [5, p. 414]

Values for flow rates are pretty much predetermined by the reservoirs' potentials; however, flow rates can be decreased by means of choking in order to avoid too big separator dimensions.

Another important input parameter of the successive equations is the diameter of the droplets, which should be separated by means of gravity. As always, the exact values vary between the various separator type and application, however, for a first stage production separator, it is in the order of magnitude of 140 micrometer upwards. [9, 154, 203]

Finally, retention times are especially important for the sizing of the separator and hence they are defined, explained and instanced in chapter 5.2 more extensively.

5.2 General Approach – Half-full Cylindrical Horizontal Three-Phase Separator

The general theory behind the sizing approach is explained by means of a cylindrical horizontal three-phase separator and is basically based on the phase separation principles, which are presented in chapter 3.3. Within that procedure, the design of the volume of a separator is determined by the gas and the liquid capacity constraints, which need to be fulfilled to keep the fluids inside as long as it is needed to achieve a sufficient separation.

The subsequent approach is based on the assumption of a half-full cylindrical horizontal three-phase separator without any of the previously described issues of chapter 4.1. Any modification for a different liquid level can of course be made and have no influence on the general procedure. As already discussed, in a two-phase separator, oil or water is present while in a three-phase separator both liquid phases need to be considered at the same time. Therefore, Table 9 shows the governing processes, which determine the respective design and hence need to be taken into account. Length and diameter are those dimensions which define a cylinder and therefore, the optimum diameter-length combination is searched within this sizing procedure.

Table 9: Considerations for Separator Capacity Determination

	Two-Phase Separator	Three-Phase Separator
Gas Capacity	Oil or Water Droplet Settling in Gas	Oil (and Water) Droplet Settling in Gas
Liquid Capacity	Oil or Water Retention Time	Oil Retention Time Water Retention Time (Oil Droplet Rising in Water) Water Droplet Settling in Oil

5.2.1 Gas Capacity

The gas capacity of a two- and three-phase separator is always determined by the settling of the liquid droplets from the gas phase to the gas-liquid interface. Since oil has a lower density than water and hence a slower settling velocity, the settling theory of oil in gas is used during the gas capacity constraint while the water settling can be skipped. The main approach in doing so is to equate the settling time of the droplet with the time the gas stays or at least should stay within the separator, called retention time, as in **eq.31**. [9, p. 205]

$$t_{l,settling} = t_{g,retention} \quad (31)$$

$t_{l,settling}$ settling time of the liquid droplet in the continuous gas phase [s]
 $t_{g,retention}$ retention time of the gas in the separator [s]

The former can be calculated by means of the settling velocity, derived in chapter 3.3, and the maximum possible distance for a liquid droplet within the gas phase in a half-full separator, namely $D/2$, the length from the uppermost to the gas-liquid interface. For the second one, the gas velocity and effective separator length is used, as shown in **eq.32**. [9, p. 208]

$$\frac{D}{2*v_{settling}} = \frac{L_{eff}}{v_g} \quad (32)$$

D	inner vessel diameter [m]
$v_{settling}$	settling velocity of the liquid droplet [m/s]
L_{eff}	effective separator length [m]
v_g	gas velocity [m/s]

Gas velocity is obviously the gas flow rate divided by the corresponding cross-sectional area as show in **eq.33**. However, gas flow rates are usually indicated at standard conditions in standard cubic meters per second, where gas behaves almost ideally. Therefore, the real gas flow rate needs to be corrected for the difference between the separator and the standard conditions of 288.15 °K and 101,325 Pa according to the Society of Petroleum Engineers (SPE) in cubic meters per hour, which is a more appropriate unit. [9, pp. 206-207]

$$v_g = \frac{Q_{g,sep} * \frac{1 h}{3600 s}}{A_g} = \frac{Q_{g,sc} * \frac{101,325 Pa}{p} * \frac{T}{288.15 °K} * Z}{\left(\frac{D^2 * \pi}{4}\right) * \frac{1}{2}} \quad (33)$$

$Q_{g,sep}$	gas flow rate at separator conditions [m ³ /h]
A_g	cross-sectional area available for gas flow [m ²]
$Q_{g,sc}$	gas flow rate at standard conditions [sm ³ /s]
p	operating pressure [Pa]
T	operating temperature [°K]
Z	gas deviation or compressibility factor [-]

After inserting **eq.26** and **eq.33** into **eq.32**, **eq.34** can then be further reduced and rearranged as shown in **eq.34**.

$$\frac{D}{2 * \sqrt{\frac{4 * d * g * (\rho_l - \rho_g)}{3 * C_D * \rho_g}}} = \frac{L_{eff}}{\frac{Q_{g,sc} * \frac{101,325 Pa}{p} * \frac{T}{288.15 °K} * Z}{\left(\frac{D^2 * \pi}{4}\right) * \frac{1}{2}}} \quad (34)$$

Eq.35 already outputs diameter-length products, which satisfy the gas capacity constraint.

$$D * L_{eff} = \frac{Q_{g,sc} * T * Z * 4}{p * \sqrt{\frac{4 * d * g * (\rho_l - \rho_g)}{3 * C_D * \rho_g}}} * \frac{101,325 Pa}{288.15 °K} * \frac{1}{\pi} \quad (35)$$

5.2.2 Liquid Capacity

The second constraint, namely the liquid capacity, includes the required retention times of oil and water to allow gas liberation and hence to reach equilibrium between the liquid and

gaseous phase. In the optimum case, the liquid stays within the separator for this amount of time to achieve ideal phase separation. Further, both water droplet settling in the oil phase and oil droplet rising in the water phase need to be considered here. Generally, the retention time of oil and water is the respective volume divided by its flow rate as shown in **eq.36** and **eq.37**. [9, pp. 267-268]

$$t_{r,o} = \frac{V_o}{Q_{o,sep}} \quad (36)$$

$t_{r,o}$	oil retention time [h]
V_o	oil volume within the separator [m ³]
$Q_{o,sep}$	oil flow rate at separator conditions [m ³ /h]

$$t_{r,w} = \frac{V_w}{Q_{w,sep}} \quad (37)$$

$t_{r,w}$	water retention time [h]
V_w	water volume within the separator [m ³]
$Q_{w,sep}$	water flow rate at separator conditions [m ³ /h]

The respective liquid phase volumes can then be written as stated in **eq.38** and **eq.39**. [9, pp. 267-268]

$$V_o = V_l * \frac{A_o}{A_l} = \frac{1}{2} * \frac{D^2 * \pi}{4} * L_{eff} \frac{A_o}{A_l} \quad (38)$$

V_l	liquid volume within the separator [m ³]
A_o	cross-sectional area available for oil flow [m ²]
A_l	cross-sectional area available for liquid flow [m ²]

$$V_w = V_l * \frac{A_w}{A_l} = \frac{1}{2} * \frac{D^2 * \pi}{4} * L_{eff} \frac{A_w}{A_l} \quad (39)$$

A_w	cross-sectional area available for water flow [m ²]
-------	---

Similar to the gas flow rates, the liquid flow rates are also indicated at standard conditions in standard cubic meters per second and therefore, they are also converted into more convenient cubic meters per hour as in **eq.40** and **eq.41**. Due to low compressibility of oil and water compared to gas, there is no need for any volume correction. [9, p. 268]

$$Q_{o,sep} = Q_{o,sc} * \frac{3600 s}{1h} \quad (40)$$

$Q_{o,sc}$ oil flow rate at standard conditions [sm^3/s]

$$Q_{w,sep} = Q_{w,sc} * \frac{3600 s}{1h} \quad (41)$$

$Q_{w,sc}$ water flow rate at standard conditions [sm^3/s]

After inserting **eq.38** and **eq.40** into **eq.36** and **eq.39** and **eq.41** into **eq.37**, **eq.42** and **eq.43** arise as results.

$$t_{r,o} = \frac{\frac{1}{2} * \frac{D^2 * \pi}{4} * L_{eff} * \frac{A_o}{A_l}}{Q_{o,sc} * \frac{3600 s}{1h}} = \frac{D^2 * \pi * L_{eff}}{Q_{o,sc} * 8} * \frac{A_o}{A_l} * \frac{1 h}{3600 s} \quad (42)$$

$$t_{r,w} = \frac{\frac{1}{2} * \frac{D^2 * \pi}{4} * L_{eff} * \frac{A_w}{A_l}}{Q_{w,sc} * \frac{3600 s}{1h}} = \frac{D^2 * \pi * L_{eff}}{Q_{w,sc} * 8} * \frac{A_w}{A_l} * \frac{1 h}{3600 s} \quad (43)$$

The sum of **eq.42** and **eq.43** and these simultaneously happening processes is then presented in **eq.44**.

$$t_{r,o} * Q_{o,sc} + t_{r,w} * Q_{w,sc} = \frac{D^2 * \pi * L_{eff}}{8} * \frac{1 h}{3600 s} * \frac{(A_o + A_w)}{A_l} \quad (44)$$

Since the cross-sectional area available for oil and water flow together are equal to the cross-sectional available for liquid flow, the last fraction in **eq.44** equals to 1. Finally, after some rearrangement, **eq.45** gives appropriate diameter-length combinations, which fulfill the liquid capacity constraint. [9, p. 269]

$$D^2 * L_{eff} = (t_{r,o} * Q_{o,sc} + t_{r,w} * Q_{w,sc}) * \frac{3600 s}{1h} * \frac{8}{\pi} \quad (45)$$

The corresponding retention times can be determined during laboratory studies and usually get higher with increasing density and viscosity. If such data is not available, it is recommended to use 3 minutes to 30 minutes for oil and 10 minutes for water, or adhere to proven guidelines as shown in Table 10. [9, p. 264]

Table 10: Recommended Oil Retention Times [9, p. 264]

°API Gravity	Minutes
Condensate	2–5
Light crude oil (30°–40°)	5–7.5
Intermediate crude oil (20°–30°)	7.5–10
Heavy crude oil (less than 20°)	10+

Further, as already displayed in Table 9, oil droplets dispersed in the water phase need to rise to the oil zone and dispersed water droplets within the oil phase have to settle down in order to achieve sufficient liquid separation, as desired in a three-phase separator. Due to the higher viscosity of the oil compared to water, the settling of water droplets in the continuous oil phase is more decisive and determining for the separator sizing and hence the only one derived here. The approach is based on a water droplet on top of the oil, which has to settle through the entire oil phase. Therefore, the oil retention time has to be sufficiently long to allow the water droplet to settle through the maximum oil pad thickness before the oil flows over the weir. This can be expressed by **eq.46**, or in other words, there is a maximum allowable oil zone thickness for the corresponding oil retention time, as shown in **eq.47**. This constraint limits the vessel diameter and hence secures a minimum effective separation length due to this upper boundary of the diameter, because **eq.35** and **eq.45** need to be fulfilled at all times. [9, pp. 267-274]

$$t_{r,o} * \frac{3600 \text{ s}}{1 \text{ h}} = \frac{h_{o,max}}{v_{settling}} \quad (46)$$

$h_{o,max}$ maximum oil pad thickness [m]

$$h_{o,max} = t_{r,o} * \frac{3600 \text{ s}}{1 \text{ h}} * v_{settling} \quad (47)$$

The geometrical relationship of the cross-sectional area available for water flow, the entire cross-sectional area of the cylindrical separator, the oil pad thickness and the vessel diameter, which are shown in Figure 31, can then be expressed by an equation, which is pictured as a graph in Figure 32. [9, p. 271]

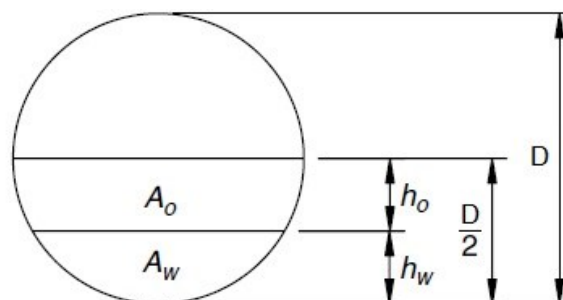


Figure 31: Geometrical Relationships in a Half-Full Cylindrical Horizontal Three-Phase Separator [9, p. 272]

However, at first, the ratio of the cross-sectional area available for water flow and the entire cross-sectional area needs to be computed in order to find the maximum allowable vessel diameter and moreover, the minimum effective separation length. Based on the assumption of a half-full cylindrical horizontal separator, the entire cross-sectional area of the pressure vessel can be written as shown in **eq.48**. After rearranging and the replacement of the cross-sectional areas by the product of flow rate and retention time, the ratio can finally be calculated with **eq.49**. [9, pp. 271-273]

$$A = 2 * (A_o + A_w) \quad (48)$$

A cross-sectional area of the cylindrical separator [m²]

$$\frac{A_w}{A} = 0.5 * \left(\frac{A_w}{A_o + A_w} \right) = 0.5 * \left(\frac{Q_{w,sep} * t_{r,w}}{Q_{o,sep} * t_{r,o} + Q_{w,sep} * t_{r,w}} \right) \quad (49)$$

With this ratio and the previously mentioned graph in Figure 32, a value for the ratio of the oil pad thickness and the vessel diameter can be read off. [8, p. 139]

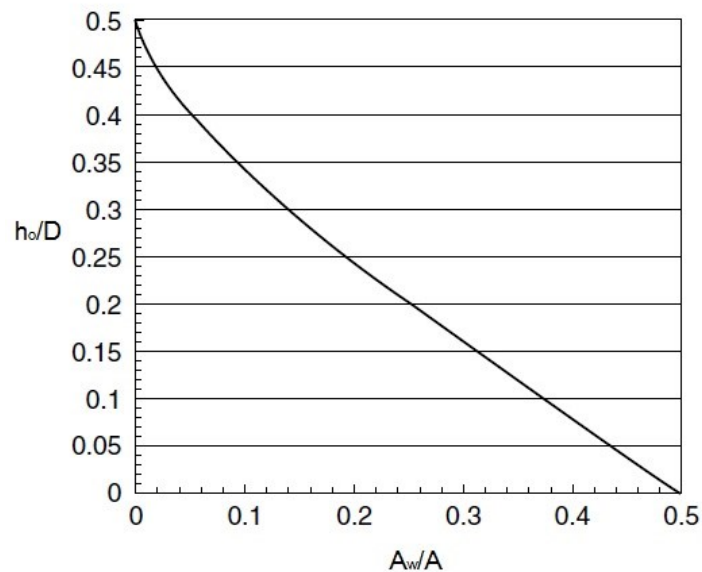


Figure 32: Relationship between h_o/D and A_w/A in a Half-Full Cylindrical Horizontal Three-Phase Separator [8, p. 140]

By means of this value and the already calculated maximum allowable oil pad thickness with **eq.47**, the maximum vessel diameter can be determined according to **eq.50**. [8, p. 139]

$$D_{max} = \frac{h_{o,max}}{\frac{h_o}{D}} \quad (50)$$

D_{max} maximum allowable separator diameter [m]

After determining the maximum permissible separator diameter, all smaller diameter are used to calculate effective separation lengths that fulfill the gas capacity constraint of **eq.35** and the liquid capacity constraint of **eq.45**. A comparison of both then reveals the governing constraint, namely the one with the larger required effective separation length at the same vessel diameter. [8, p. 142]

5.2.3 Seam-to-Seam Length

The so-called seam-to-seam lengths are then calculated with all the allowable effective separation lengths of the prevailing capacity constraint. **Eq.51** is used if the gas capacity constraint is more dominant while **eq.52** is applied in the case of a governing liquid capacity. [8, p. 142, 9, p. 277]

$$L_{ss} = L_{eff} + D \quad (51)$$

L_{ss} seam-to-seam length of the separator [m]

$$L_{ss} = \frac{4}{3} * L_{eff} \quad (52)$$

5.2.4 Slenderness Ratio

The final selection of seam-to-seam length and vessel diameter is then made based on the ratio of those two parameters, called the slenderness ratio. Experience shows that values between 3 to 5 are most favorable and hence are recommended. In order to save costs and avoid special constructions, it is advocated to follow the standardized vessel sizes according to API Specification 12J. [8, p. 142, 9, p. 278]

5.3 API Specification and ASME Code

In general, most of the countries follow the minimum requirements for the design and manufacture of oil and gas separators, which are explicitly documented in the Specification 12J by the American Petroleum Institute. Fee-based guidelines for the whole design procedure are available online. Further, it also refers to the American Society of Mechanical Engineers' Boiler and Pressure Vessel Code for the mechanical design aspects and material requirements. Especially Division 1 of Section VIII is most commonly used since it covers pressure vessels with operating pressures above 15 psig. [9, 316, 319]

After determining the separator's length and diameter, the wall thickness is calculated according to the ASME Code, as shown in Figure 33. Following the material selection, which should be capable of withstanding the operating conditions including a safety factor of 3.5 as per Division 1, the weight and hence the costs of the pressure vessel are calculated. [9, pp. 319-320]


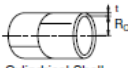



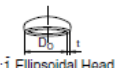



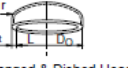
FORMULAS FOR VESSELS UNDER INTERNAL PRESSURE																																					
<p>NOTATION</p> <p>α = Half Apex Angle of Cone, Deg.</p> <p>D = Inside diameter, inches</p> <p>D_o = Outside diameter, inches</p> <p>E = Efficiency of welded joints</p> <p>L = Inside crown radius, inches</p> <p>L_o = Outside crown radius, inches</p> <p>M = Factor, see table below</p> <p>P = Design pressure or maximum allowable pressure, psig</p>																																					
In Terms INSIDE Radius or Diameter	In Terms OUTSIDE Radius or Diameter																																				
 $t = \frac{PR}{SE - 0.6P}$ $P = \frac{SEt}{R + 0.6t}$ <p>Cylindrical Shell Formulas for Longitudinal seam</p>	 $t = \frac{PR_o}{SE + 0.4P}$ $P = \frac{SEt}{R_o + 0.4t}$ <p>Cylindrical Shell Formulas for Longitudinal seam</p>																																				
 $t = \frac{PR}{2SE - 0.2P}$ $P = \frac{2SEt}{R + 0.2t}$ <p>Sphere Hemispherical Head</p>	 $t = \frac{PR_o}{2SE - 0.8P}$ $P = \frac{2SEt}{R_o + 0.8t}$ <p>Sphere Hemispherical Head</p>																																				
 $t = \frac{PD}{2SE - 0.2P}$ $P = \frac{2SEt}{D + 0.2t}$ <p>2:1 Ellipsoidal Head</p>	 $t = \frac{PD_o}{2SE - 1.8P}$ $P = \frac{2SEt}{D_o + 1.8t}$ <p>2:1 Ellipsoidal Head</p>																																				
 $t = \frac{PD}{2 \cos \alpha (SE - 0.6P)}$ $P = \frac{2SEt \cos \alpha}{D + 1.2t \cos \alpha}$ <p>Cone & Conical Section α Maximum = 30 Deg.</p>	 $t = \frac{PD_o}{2 \cos \alpha (SE - 0.4P)}$ $P = \frac{2SEt \cos \alpha}{D_o + 1.8t \cos \alpha}$ <p>Cone & Conical Section α Maximum = 30 Deg.</p>																																				
 $t = \frac{PLM}{2SE - 0.2P}$ $P = \frac{2SEt}{LM + 0.2t}$ <p>Flanged & Dished Head</p>	 $t = \frac{PL_oM}{2SE + P(M - 0.2)}$ $P = \frac{2SEt}{ML_o - t(M - 0.2)}$ <p>Flanged & Dished Head</p>																																				
<table border="1"> <tr> <td>FACTOR</td> <td>L/t</td> <td>6.5</td> <td>7.5</td> <td>8.0</td> <td>8.5</td> <td>9.0</td> <td>9.5</td> <td>10.00</td> <td>10.5</td> <td>11.0</td> <td>11.5</td> <td>12.00</td> <td>13.0</td> <td>14.0</td> <td>15.0</td> <td>16.0</td> <td>16.67</td> </tr> <tr> <td>M</td> <td>M</td> <td>1.39</td> <td>1.41</td> <td>1.44</td> <td>1.46</td> <td>1.50</td> <td>1.52</td> <td>1.54</td> <td>1.56</td> <td>1.58</td> <td>1.60</td> <td>1.62</td> <td>1.65</td> <td>1.69</td> <td>1.72</td> <td>1.75</td> <td>1.77</td> </tr> </table>	FACTOR	L/t	6.5	7.5	8.0	8.5	9.0	9.5	10.00	10.5	11.0	11.5	12.00	13.0	14.0	15.0	16.0	16.67	M	M	1.39	1.41	1.44	1.46	1.50	1.52	1.54	1.56	1.58	1.60	1.62	1.65	1.69	1.72	1.75	1.77	
FACTOR	L/t	6.5	7.5	8.0	8.5	9.0	9.5	10.00	10.5	11.0	11.5	12.00	13.0	14.0	15.0	16.0	16.67																				
M	M	1.39	1.41	1.44	1.46	1.50	1.52	1.54	1.56	1.58	1.60	1.62	1.65	1.69	1.72	1.75	1.77																				
<p>PRESSURE VESSEL HANDBOOK PUBLISHING, INC.</p> <p>P.O. BOX 35365 - TULSA, OK. 74153-0365</p>																																					

Figure 33: Wall Thickness Determination According to the ASME Code [9, p. 322]

6 HSE

Proper planning, design and fabrication usually assure safe activities and this is the key to operating in an environmentally friendly way. Nevertheless, one should always be prepared for the worst case because health, safety and environment should be the most important at all times. In addition to the performance enhancing internals, which are explained in chapter 3.4, some components are built-in if something unwanted happens.

6.1 Safety Elements

On the one hand, high-level controls, mentioned in chapter 4.1.3, shut in the inlet and activate a bypass while making an alert signal in case of a too high interface or liquid level inside the separator. On the other hand, low-level controls, introduced in chapter 4.1.4, either shut in the inlet or outlet and also signal a warning. [8, p. 88, 9, p. 193]

Furthermore, mechanically, pneumatically or electrically steered pressure controls close the inlet and bypass the fluids in order to maintain constant operating pressure. Besides pressure, temperature is also continuously monitored to shut down the operation if the temperature undercuts or exceeds certain limits, which are respectively governed by the wax appearance temperature and the material of the internals and the shell of the pressure vessel. [8, pp. 88-89, 9, 192, 317]

A spring-loaded safety relief valve with its discharge line is then the second last resort in the event of a too high internal pressure. It is adjusted to the upper limit of the pressure control and opens only at even higher pressures. If everything fails and the pressure further increases, a thin membrane out of metal, called safety head or rupture disk, breaks and releases the pressure via another discharge line. [8, p. 89, 9, p. 342]

6.2 Waste Management

Along with the oil and gas, water and solids are usually produced and hence need to be safely disposed. It is either produced formation water or flow back water from stimulation or injection jobs and contains inorganic and organic constituents. The former are dissolved salts, traces of metals, chemicals introduced by the human being, natural occurring radioactive materials (NORM) or other ions, which could precipitate as pressure and temperature decrease. Latter are simply hydrocarbons, which are either dissolved or dispersed within the water phase. After leaving the three-phase separator and prior to the final disposal, the water needs to be treated and cleaned by means of filtration, cyclonic separation, flotation or even evaporation. [12, pp. 6-7]

The second big group of waste, which accumulates during oil and gas production and separation, is sand. It is usually removed through the drains, presented in chapter 3.4.3, and has to be cleaned from hydrocarbons before finally dumping it. Contamination of sand is measured in Total Organic Content (TOC) and a combination of mechanical washing and ultrasonic technology can remove up to 99.5%, which is referred to as the most effective

cleaning process. It is also very reliable, safe and environmentally friendly since no chemicals are needed during this procedure. [13, 1, 6-11]

7 Computational Fluid Dynamics Modeling

The field of computational fluid dynamics deals with the analysis of fluid flow, in consideration of the physical properties. Especially the flow behavior in newly designed elements, components or devices is often modeled and analyzed on the computer before such parts are really manufactured. ANSYS Fluent and OpenFOAM are just two examples of many software available on the market and CFD get more and more attention in all industries due to the trend towards interdisciplinary work. Of course, one always has to assess and appraise if the present problem and task is worth being analyzed in regards to fluid dynamics.

In this chapter, the application of computational fluid dynamics is demonstrated based on a horizontal three-phase separator using OpenFOAM, a free, open-source CFD software. A simulation is able to give insights into the behavior inside the vessel, reveals possible critical parts and areas of the system and analytical calculations can be checked if the input parameters, as chosen retention times, are appropriate and sufficient.

7.1 Analytical Calculation

Based on chapter 5.2, sizing of a half-full cylindrical horizontal three-phase separator is done by analytical calculations. The input parameters, which are also used in the numerical approach afterward, are shown in Table 11 and are either randomly chosen within realistic ranges, average values or based on experience, for example Table 10.

Table 11: Input Parameters

phase fraction gas	α_g	0.5	-
phase fraction oil	α_o	0.2	-
phase fraction water	α_w	0.3	-
droplet diameter	d	0.001	m
gas density	ρ_g	17.585	kg/m ³
oil density	ρ_o	813	kg/m ³
water density	ρ_w	1015	kg/m ³
drag coefficient	C_D	1	-
inlet diameter	d_{inlet}	0.4	m
inlet velocity	v_{inlet}	0.2	m/s
oil retention time	$t_{r,o}$	0.073	h
water retention time	$t_{r,w}$	0.167	h

The first step is the computation of the gas and liquid capacity constraints, respectively shown in **eq.35** and **eq.45** before, and conducted in **eq.53** and **eq.54**.

$$D * L_{eff} = \frac{Q_{g,sc} * T * Z * 4}{p * \sqrt{\frac{4 * d * g * (\rho_l - \rho_g)}{3 * C_D * \rho_g}}} * \frac{101,325 \text{ Pa}}{288.15 \text{ }^\circ\text{K}} * \frac{1}{\pi} = \frac{A_{inlet} * \alpha_w * v_{inlet} * \frac{3600s}{1h} * 4}{\sqrt{\frac{4 * d * g * (\rho_l - \rho_g)}{3 * C_D * \rho_g}}} * \frac{1}{\pi} = \frac{\frac{d_{inlet}^2 * \pi}{4} * \alpha_g * v_{inlet} * \frac{3600s}{1h} * 4}{\sqrt{\frac{4 * d * g * (\rho_l - \rho_g)}{3 * C_D * \rho_g}}} * \frac{1}{\pi} = 18.7 \text{ m}^2 \quad (53)$$

$$D^2 * L_{eff} = (t_{r,o} * Q_{o,sc} + t_{r,w} * Q_{w,sc}) * \frac{3600 \text{ s}}{1h} * \frac{8}{\pi} = \left(t_{r,o} * \frac{d_{inlet}^2 * \pi}{4} * \alpha_o * v_{inlet} + t_{r,w} * \frac{d_{inlet}^2 * \pi}{4} * \alpha_w * v_{inlet} \right) * \frac{3600 \text{ s}}{1h} * \frac{8}{\pi} = 14.88 \text{ m}^3 \quad (54)$$

Second, the maximum oil pad thickness is obtained by inserting **eq.27** and the required input parameters into **eq.47**, as shown in **eq.55**.

$$h_{o,max} = t_{r,o} * \frac{3600 \text{ s}}{1h} * v_{settling} = t_{r,o} * \frac{3600 \text{ s}}{1h} * \sqrt{\frac{4 * d * g * (\rho_w - \rho_o)}{3 * C_D * \rho_o}} = 0.073 \text{ h} * \frac{3600 \text{ s}}{1h} * \sqrt{\frac{4 * 0.001 \text{ m} * 9.81 \frac{\text{m}}{\text{s}^2} * (1015 \frac{\text{kg}}{\text{m}^3} - 813 \frac{\text{kg}}{\text{m}^3})}{3 * 1 * 813 \frac{\text{kg}}{\text{m}^3}}} = 14.96 \text{ m} \quad (55)$$

Eq.49 is then utilized as shown in **eq.56** and the output is used in Figure 32 to read off the ratio of oil pad thickness to inner vessel diameter in order to calculate the maximum allowable separator diameter, defined by **eq.50**.

$$\frac{A_w}{A} = 0.5 * \left(\frac{Q_{w,sep} * t_{r,w}}{Q_{o,sep} * t_{r,o} + Q_{w,sep} * t_{r,w}} \right) = 0.5 * \left(\frac{A_{inlet} * \alpha_w * v_{inlet} * \frac{3600s}{h} * 0.167 \text{ h}}{\frac{3600s}{h} * 0.073 \text{ h} + A_{inlet} * \alpha_w * v_{inlet} * \frac{3600s}{h} * 0.167 \text{ h}} \right) = 0.5 * \left(\frac{\frac{d_{inlet}^2 * \pi}{4} * \alpha_w * v_{inlet} * \frac{3600s}{h} * 0.167 \text{ h}}{\frac{d_{inlet}^2 * \pi}{4} * \alpha_o * v_{inlet} * \frac{3600s}{h} * 0.073 \text{ h} + \frac{d_{inlet}^2 * \pi}{4} * \alpha_w * v_{inlet} * \frac{3600s}{h} * 0.167 \text{ h}} \right) = 0.5 * \left(\frac{\frac{(0.4\text{m})^2 * \pi}{4} * 0.3 * 0.2 \frac{\text{m}}{\text{s}} * \frac{3600s}{h} * 0.167 \text{ h}}{\frac{(0.4\text{m})^2 * \pi}{4} * 0.2 * 0.2 \frac{\text{m}}{\text{s}} * \frac{3600s}{h} * 0.073 \text{ h} + \frac{(0.4\text{m})^2 * \pi}{4} * 0.3 * 0.2 \frac{\text{m}}{\text{s}} * \frac{3600s}{h} * 0.167 \text{ h}} \right) = 0.387 \quad (56)$$

The corresponding ratio of oil pad thickness to an inner vessel diameter of 0.08 and the previously calculated maximum oil pad thickness lead then to a maximum allowable separator diameter as shown in **eq.57**.

$$D_{max} = \frac{h_{o,max}}{\frac{h_o}{D}} = \frac{14.96 \text{ m}}{0.08} = 187 \text{ m} \quad (57)$$

Afterward, all diameters smaller than the maximum are used to calculate corresponding effective lengths which fulfill the gas capacity constraint and the liquid capacity constraint. The higher effective length for the same diameter then reveals the governing constraint. In this example, not all vessel inner diameters smaller than 187 m are used but smaller than 10 m, which is more realistic. The results, presented in Table 12 below, show that the gas capacity constraint is determining and hence, used for the effective length selection.

Table 12: Diameter - Length Combinations

Gas Capacity Constraint				Liquid Capacity Constraint			
D	m	L _{eff}	m	D	m	L _{eff}	m
10	m	1.9	m	10	m	0.15	m
9.5	m	2	m	9.5	m	0.16	m
9	m	2.1	m	9	m	0.18	m
8.5	m	2.2	m	8.5	m	0.21	m
8	m	2.3	m	8	m	0.23	m
7.5	m	2.5	m	7.5	m	0.26	m
7	m	2.7	m	7	m	0.30	m
6.5	m	2.9	m	6.5	m	0.35	m
6	m	3.1	m	6	m	0.41	m
5.5	m	3.4	m	5.5	m	0.49	m
5	m	3.7	m	5	m	0.60	m
4.5	m	4.2	m	4.5	m	0.73	m
4	m	4.7	m	4	m	0.93	m
3.5	m	5.3	m	3.5	m	1.21	m
3	m	6.2	m	3	m	1.65	m
2.5	m	7.5	m	2.5	m	2.38	m
2	m	9.4	m	2	m	3.72	m
1.5	m	12.5	m	1.5	m	6.61	m
1	m	18.7	m	1	m	14.88	m
0.5	m	37.4	m	0.5	m	59.52	m

As the last step, **eq.51** is used to calculate the seam-to-seam length possibilities of the separator, which are then taken for the slenderness ratios. Since it is recommended that latter is between 3 and 5, the inner vessel diameter of 2.5 m, the effective separation length of 7.5 m, the seam-to-seam length of 10 m and the slenderness ratio of 4 is chosen, as highlighted in Table 13.

Table 13: Seam-to-Seam Lengths and Slenderness Ratios

Gas Capacity Constraint							
D	m	L_{eff}	m	L_{ss}	m	Ratio	-
10	m	1.9	m	11.9	m	1.19	-
9.5	m	2	m	11.5	m	1.21	-
9	m	2.1	m	11.1	m	1.23	-
8.5	m	2.2	m	10.7	m	1.26	-
8	m	2.3	m	10.3	m	1.29	-
7.5	m	2.5	m	10.0	m	1.33	-
7	m	2.7	m	9.7	m	1.38	-
6.5	m	2.9	m	9.4	m	1.44	-
6	m	3.1	m	9.1	m	1.52	-
5.5	m	3.4	m	8.9	m	1.62	-
5	m	3.7	m	8.7	m	1.75	-
4.5	m	4.2	m	8.7	m	1.92	-
4	m	4.7	m	8.7	m	2.17	-
3.5	m	5.3	m	8.8	m	2.53	-
3	m	6.2	m	9.2	m	3.08	-
2.5	m	7.5	m	10.0	m	4.00	-
2	m	9.4	m	11.4	m	5.68	-
1.5	m	12.5	m	14.0	m	9.32	-
1	m	18.7	m	19.7	m	19.72	-
0.5	m	37.4	m	37.9	m	75.88	-

7.2 Numerical Approach

As already mentioned, the input parameters of the analytical procedure are used in the numerical approach as well. Further, the recommended separator dimensions are also tested, and an engineering drawing of the separator geometry is shown in Figure 34.

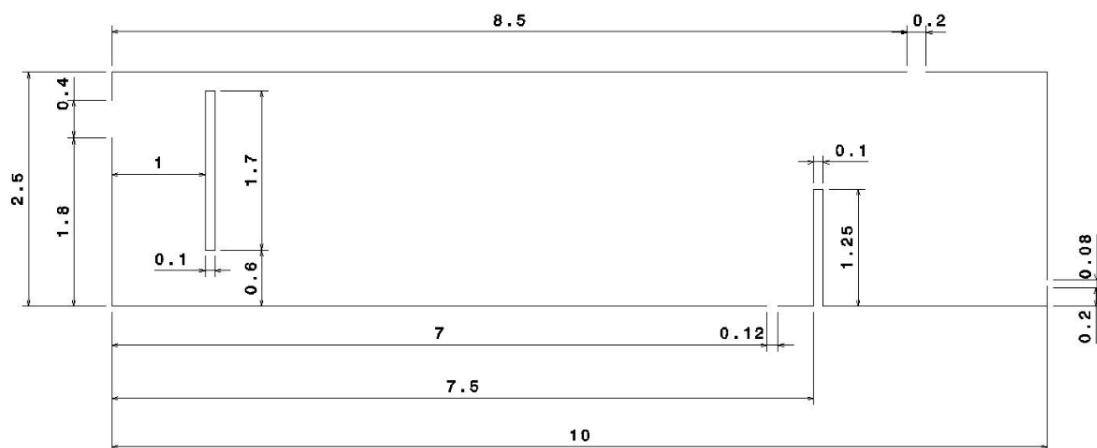


Figure 34: Engineering Drawing of the Separator Geometry in Meters

While the computation itself can be done in OpenFOAM, the pre-processing including the generation of the geometry and the mesh is better conducted in SALOME, as respectively shown in Figure 35 and Figure 36. Only for very simple cases, it is feasible to perform the meshing directly in OpenFOAM. The geometry and mesh only represent the inner volume of the separator available for fluid flow. Thus down comer inlet diverter, which acts at low inlet velocities as a wave breaker only, and weir are excluded, as depicted in Figure 35.

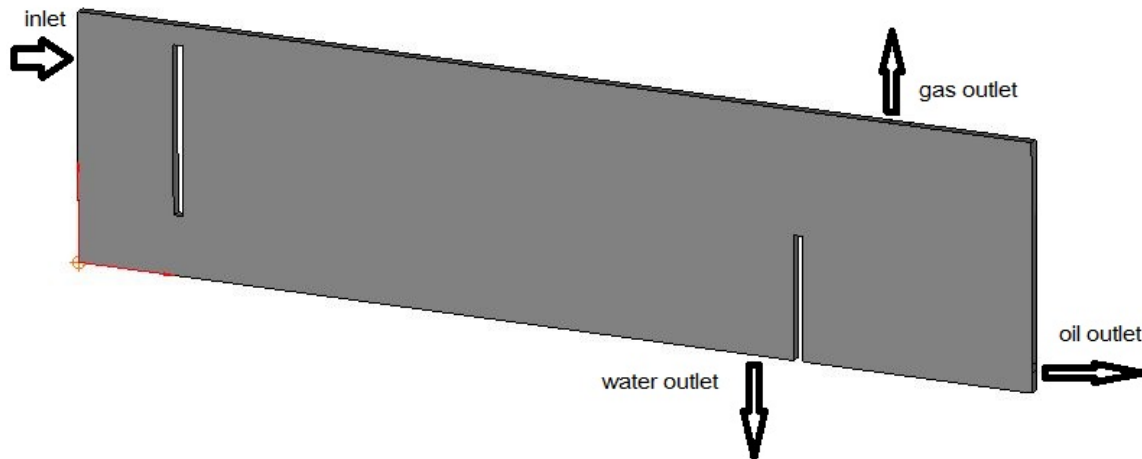


Figure 35: Geometry of the Separator in SALOME

As highlighted in Figure 36, a three-dimensional mesh needs to be created and is also required by OpenFOAM, even though the simulation is two-dimensional. This can be achieved by extruding a 2D triangular mesh, previously generated on the front face, with one cell in direction of the third dimension. Cell size can be estimated by means of the so-called Courant–Friedrichs–Lewy condition, or short Courant Number, as stated in **eq.58**. Fluid movement from one cell to another within a single time step results in a Courant Number less than 1, which should be the case at all times. [14]

$$C = \frac{u \cdot \Delta t}{\Delta x} \quad (58)$$

C	Courant Number [-]
u	magnitude of the velocity [m/s]
Δt	time step [s]
Δx	length interval [m]

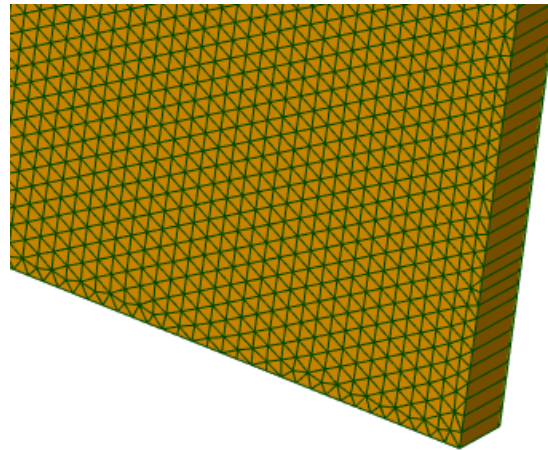


Figure 36: Detailed View of the Triangular Mesh of the Separator in SALOME

It is necessary to create mesh groups called patches, see the *boundary* file in OpenFOAM later on, to define appropriate physical boundary conditions. The inlet, through which the mixture flows into the separator, the gas outlet, the oil outlet and the water outlet, through which the respective phases flow out of the vessel, the wall, the front and the back. The mesh can be exported into UNV-format and directly copied into the OpenFOAM project folder. By means of *ideasUnvToFoam*, the mesh is converted to foam-format and a new *polyMesh* folder in the *constant* directory is created.

Since triangular cells are problematic when the direction of the fluid movement is not known, the mesh is converted to a polyhedral one, as shown in Figure 37, by means of the *polyDualMesh* utility. It also reduces the number of cells drastically, which saves a lot of computation time. The *constant* folder, which is the model control directory, is only read once at the beginning of the simulation and includes not only the *polyMesh* folder, where the computational mesh is located, but also the gravity g and the model properties as *motionProperties*, *transportProperties* and *turbulenceProperties*.

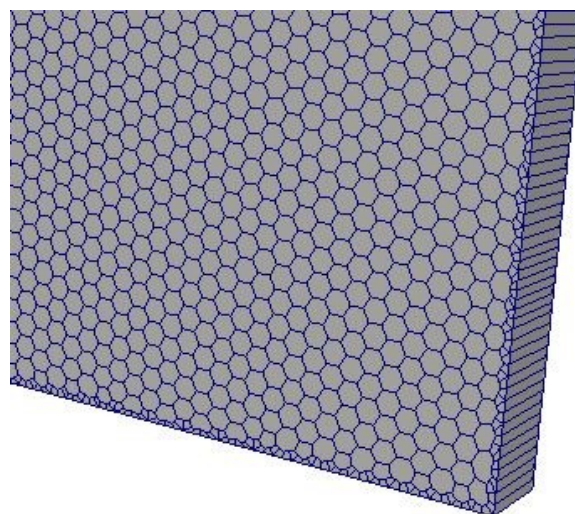


Figure 37: Detailed View of the Polyhedral Mesh of the Separator in ParaView

Basic patch types are assigned to the already mentioned patches in the *boundary* file in the *polyMesh* folder, namely Inlet: patch, GasOutlet: patch, OilOutlet: patch, WaterOutlet: patch, Wall: patch and Front and Back empty, since there is no solution required in the third dimension.

The *simulationType* in *turbulenceProperties* should be set to laminar since turbulences disturb the separation in the pressure vessel and therefore, they should not be present. Further, a static mesh can be used, as regulated in the *motionProperties*. The *transportProperties* include the fluid properties shown in Table 11 and the interfacial tension of gas and water of 0.072 N/m and of gas and oil of 0.02 N/m, which are responsible for a proper separation with an interface tracking. Latter is not tracked between oil and water and hence they can coexist as an Eulerian mixture. Only the drag coefficient is not included as in the analytical approach but represented by the *SchillerNaumann* drag model.

In the folder *0*, initial conditions like pressure, velocity and phase fractions, which are used for the calculations, can then be set. Additional field value folders are created for every iteration or time step during the computation.

Concerning velocity, the gas, oil and water *internalField* is initially set to zero while the *boundaryField* is set to a *fixedValue* of 0.2 m/s of Table 11 for the gas, oil and water inlet and the oil and water outlets. At the wall, the velocity is zero. The front and back boundaries are not solved and hence empty. The gas outlet is set to *fluxCorrectedVelocity* because we specify the value of pressure at the same location later on.

The pressure *internalField* is set to atmospheric pressure, the *boundaryField* for the inlet, wall, oil outlet and water outlet to *fixedFluxPressure* since the velocities are already prescribed there. Front and back are again empty. The gas outlet, where subsonic compressible flow occurs, is set to *totalPressure* equal to atmospheric pressure, which is corrected by the dynamic pressure.

The inlet *boundaryField* of the phase fractions is set to *fixedValue* 0.5 for gas, 0.2 for oil and 0.3 for water, according to Table 11. The outlets are set to *InletOutlet* to prevent backflow with value 1 for the corresponding phase and value 0 for the undesired phases. Wall is set to *zeroGradient* while front and back are again empty. The *internalField* is set by means of an initialization scheme that can be seen in Figure 38, Figure 39 and Figure 40. A phase fraction of 1 represents a pure phase while a value of 0 means that this phase does not occur at this position. It is important to mention that the sum of all phase fractions at the same location has to add up to 1 at all times.



Figure 38: Phase Fraction of Gas at the Beginning

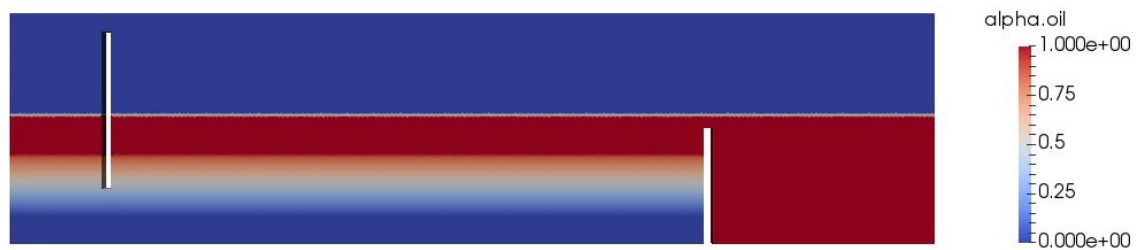


Figure 39: Phase Fraction of Oil at the Beginning

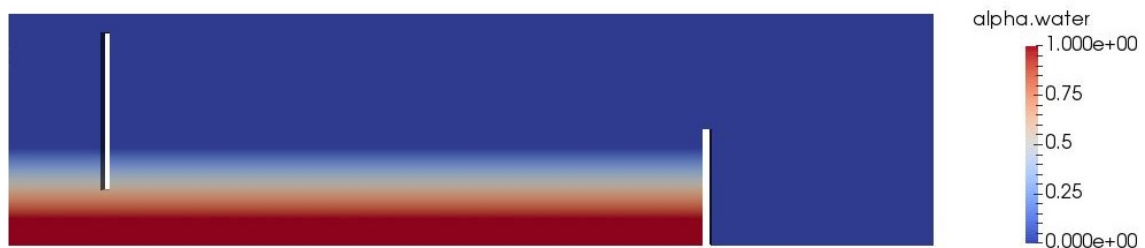


Figure 40: Phase Fraction of Water at the Beginning

The *system* folder, where all criteria associated with the solution of the problem itself are adjusted, is re-read at every iteration or time step. Due to the presence of two incompressible and one compressible phases, the *multiphaseEulerFoam* is selected in the *controlDict*, being a solver for a system of many compressible fluid phases. The conservation laws, together with constitutive relations form a closed system of non-linear partial differential equations, called Navier-Stokes equations, which are solved for every phase.

Furthermore, in *controlDict*, the time step, which satisfies the Courant–Friedrichs–Lewy condition, can be set and there is also the possibility to activate *adjustTimeStep* in order to force the Courant Number to stay below 0.6, which was set as the maximum here.

Since the *multiphaseEulerFoam* does not support the steady-state temporal differencing scheme, the explicit forward *Euler* differencing is selected in *fvSchemes*, showing the best results. The *gradSchemes* are set to *cellMDLimited Gauss linear 1* in order to additionally

stabilize the calculation of the gradients in the multiphase flow. The divergence schemes that influence the advection of the phase fractions are set to *Gauss vanLeer*, which leads to the least residuals and continuity fluctuations, while the schemes that affect the velocity fields are set to *Gauss limitedLinear 1*. These limiting schemes also help a lot with the numerical stability.

PISO algorithm, which solves the Navier-Stokes equations in unsteady problems like this, is used in *fvSolution*.

Finally, the post-processing is done in ParaView, as shown in Figure 41, 42, 43, 44 and 45. To conclude everything, the analytical calculations could be confirmed by the CFD simulation with the used input parameters. The separation takes place without any undesired fluid outflow through a wrong outlet as it happened during a test run at 1 m/s inlet velocity. A parametric study of different velocities could increase the efficiency of the separator if proper separation at an inlet velocity higher than recommended in the analytical calculations can be confirmed by the simulation. Since 1 second of the simulation took more than an hour to calculate in OpenFOAM, this is very time-consuming, but might be worth it for companies in order to achieve a higher throughput in the end.



Figure 41: Phase Fraction of Gas



Figure 42: Phase Fraction of Oil



Figure 43: Phase Fraction of Water

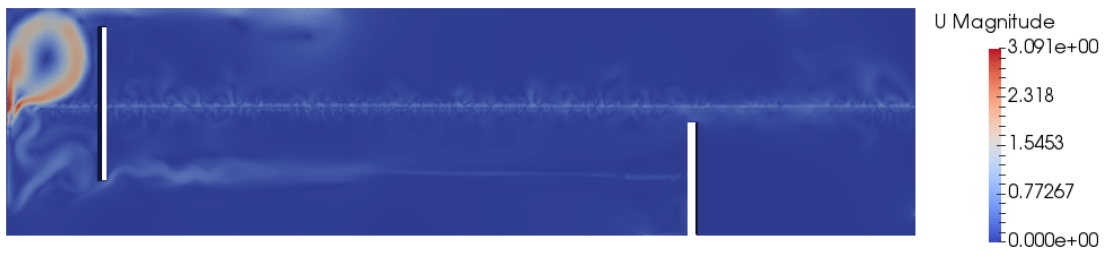


Figure 44: Total Velocity in Meters per Second



Figure 45: Densities in Kilogram per Cubic Meter

8 Conclusion

The design of a separator is a very extensive and stepwise procedure, which is summarized in Figure 46. Overall, the most important thing is knowledge about the entire system and the present case, which is most likely a unique one. This starts with the determination of the characteristics, composition and fluid properties of the crude petroleum, water and other impurities in the mixed well stream. Additionally, the phase behaviors need to be clearly understood for the phase separation afterward. Fluid samples are sources, that are more reliable than mathematical approaches and therefore, they are crucial in order to come up with valid input parameters, which are the basis for a proper result of the design in the end. The detailed application and configuration for the desired task and function of the separator needs to be clarified in advance and for this and the present media, the ideal operating conditions need to be determined in the laboratory.

All these parameters are then considered and included in the sizing procedure of the pressure vessel and its inlet, gravity settling, liquid collection and mist extraction sections. As presented in detail, this process is based on the gas and liquid capacities and governed by the droplet settling theory and liquid retention times. While the former can still be perfectly described by Archimedes' Principle and Stokes' Law, the latter need to be estimated in the laboratory, measured in a test separator or determined by means of particle tracking in computational fluid dynamics simulations. With the seam-to-seam length and diameter, being the outcome of the sizing and the defining dimensions, the wall thickness of the pressure vessel can then be designed according to the ASME code.

Sloshing and slugs, foaming, liquid carry-over, gas carry-under, wax appearance, sand, corrosion and emulsions are all possible issues, which can occur during the lifetime of the field and the separator. Therefore, it is important to prevent or at least counteract and mitigate the effects of those undesired happenings by means of internals. Health, safety and environment, including safety elements and waste management of the accruing and undesired byproducts, have to be considered as well.

To sum up, the motto Garbage In, Garbage Out, mentioned at the very beginning, definitely applies to the separator design and therefore, it is essential to determine and define all the input parameters as good as possible at the start. Computational fluid dynamics is a strong design tool that can be used to optimize and improve the separator design and the efficiency of the separator itself. On the one hand, open-source software solutions as SALOME, OpenFOAM and ParaView can be used, however, high expertise is required to implement all the details in order to come up with useful and insightful results. On the other hand, commercial programs as ANSYS would be simpler for companies to use, since an ANSYS training center is available for support.

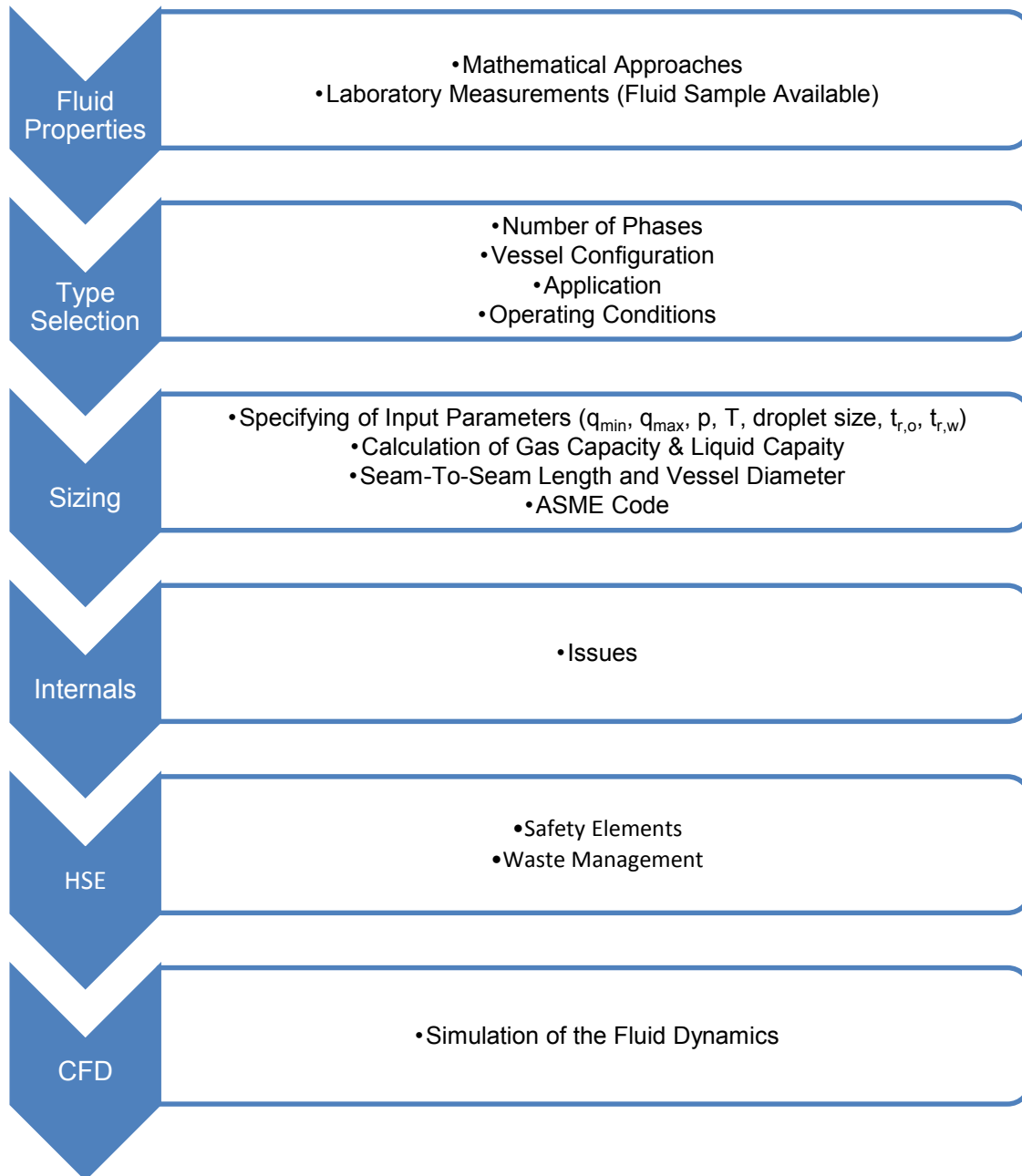


Figure 46: Overview of a Separator Design

References

- [1] Organization of the Petroleum Exporting Countries, “2017 OPEC World Oil Outlook,” A-1010 Vienna, Austria, 2017. [Online] Available: <http://www.opec.org>. Accessed on: Apr. 14 2018.
- [2] BP, *Statistical Review of World Energy*. [Online] Available: <https://www.bp.com/en/global/corporate/energy-economics/statistical-review-of-world-energy>. Accessed on: Nov. 14 2018.
- [3] M. J. Economides, *Petroleum production systems*, 2nd ed. Upper Saddle River, NJ: Prentice Hall, 2013.
- [4] www.offshoreengineering.com, *Hydrocarbon Formation*. [Online] Available: <https://wattsupwiththat.com/2017/02/18/oil-where-did-it-come-from/>. Accessed on: Nov. 14 2018.
- [5] A. Y. Dandekar, Ed., *Petroleum reservoir rock and fluid properties*, 2nd ed. Boca Raton, Fla.: CRC Press, 2013.
- [6] Wintershall Holding GmbH, *Elements of Oil*. [Online] Available: <https://www.wintershall.com/crude-oil-natural-gas/crude-oil.html>. Accessed on: Nov. 14 2018.
- [7] [petroleum.co.uk](http://www.petroleum.co.uk), *API Gravity*. [Online] Available: <http://www.petroleum.co.uk/api>. Accessed on: Nov. 14 2018.
- [8] H. K. Abdel-Aal, M. Aggour, and M. A. Fahim, *Petroleum and Gas Field Processing*. New York: Marcel Dekker, 2003.
- [9] Maurice Stewart, Ken E. Arnold, *Surface Production Operations*: Elsevier, 2016.
- [10] Schlumberger, *free-water knockout - Schlumberger Oilfield Glossary*. [Online] Available: https://www.glossary.oilfield.slb.com/Terms/f/free-water_knockout.aspx. Accessed on: Nov. 15 2018.
- [11] SPE International, *PetroWiki - Oil and Gas Separators*. [Online] Available: https://petrowiki.org/Oil_and_gas_separators#Sloshing. Accessed on: Nov. 16 2018.
- [12] World Bank Group, “Environmental, Health, and Safety Guidelines for Offshore Oil and Gas Development,” 2015.
- [13] Yiwen Xu, Clemens Langbauer, Herbert Hofstätter, *SPE-185261-MS: The Application of Ultrasonic Technology for Cleaning Oil Contaminated Sand*.
- [14] t. f. e. Wikipedia, *Courant–Friedrichs–Lewy condition*. [Online] Available: https://en.wikipedia.org/wiki/Courant%E2%80%93Friedrichs%E2%80%93Lewy_condition. Accessed on: 2019.

List of Tables

Table 1: World Population in Millions [1, p. 7]	1
Table 2: World Energy Demand in mboe/d [1, p. 9]	1
Table 3: World Energy Demand by Fuel Type [1, p. 66]	2
Table 4: Crude Oil Classification according to °API [7]	8
Table 5: Gibbs' Phase Rule [5, pp. 287-304]	9
Table 6: Classification of Reservoir Fluids [5, p. 314]	13
Table 7: Classification of Separators	24
Table 8: Characteristics and Comparison of Impingement Type Mist Extractors [9, p. 188]..	37
Table 9: Considerations for Separator Capacity Determination	44
Table 10: Recommended Oil Retention Times [9, p. 264].....	48
Table 11: Input Parameters	54
Table 12: Diameter - Length Combinations	56
Table 13: Seam-to-Seam Lengths and Slenderness Ratios	57

List of Figures

Figure 1: Reserves to Production Ratios over the Last Years (Oil left and Gas right) [2]	2
Figure 2: Petroleum Production System [3, p. 12].....	3
Figure 3: Oil and Gas Window [4].....	4
Figure 4: Elements of Crude Oil in Percentage [6].....	6
Figure 5: Organic Compounds in Crude Petroleum	7
Figure 6: Phase Diagram of a Pure Component [5, p. 288]	10
Figure 7: Phase Diagram of a Binary System [5, p. 295]	12
Figure 8: Critical Locus of a Binary System [5, p. 302].....	12
Figure 9: Typical Phase Diagram of Black Oil (left) [5, p. 312] and Volatile Oil (right) [5, p. 315].....	14
Figure 10: Typical Phase Diagram of Gas Condensate [5, p. 316]	14
Figure 11: Typical Phase Diagram of Wet Gas (left) [5, p. 318] and Dry Gas (right) [5, p. 319]	15
Figure 12: Behavior of the Phase Compositions in the Two-Phase Region of a Black Oil System [5, p. 320]	16
Figure 13: Phase Densities of a Black Oil System below the Bubble Point [5, p. 321]	16
Figure 14: Equilibrium Ratios versus Pressure at a Temperature below the Critical One [5, p. 448].....	20
Figure 15: Flow Pattern of a PVT Analysis [5, p. 364].....	21
Figure 16: Constant Composition Expansion Test of a Gas Condensate [5, p. 400].....	22
Figure 17: Differential Liberation Test of an Oil [5, p. 402]	23
Figure 18: Constant Volume Depletion Test of a Gas Condensate [5, p. 405]	23
Figure 19: Cross Section of a Typical Vertical Two-Phase Separator [9, p. 157]	25
Figure 20: Cross Section of a Typical Horizontal Two-Phase Separator [9, p. 155]	26
Figure 21: Force Equilibrium of a Heavier Phase in a Lighter Continuous Phase	28
Figure 22: Force Equilibrium of a Lighter Phase in a Heavier Continuous Phase	31
Figure 23: Cross Section of a Typical Horizontal Three-Phase Separator [9, p. 246].....	32
Figure 24: Baffle Plate Diverters - Spherical Dish (left) and Flat Plate (right) [9, p. 169]	32
Figure 25: Down Comer Inlet Diverter [9, p. 247].....	33
Figure 26: Defoaming Plates [9, p. 173]	34

Figure 27: Sand Jets and Drains [9, p. 175].....	35
Figure 28: Liquid Droplet Capture Mechanisms in a Mist Extractor [9, p. 177].....	36
Figure 29: Determination of the Optimum Operating Conditions based on Oil Gravity and Gas Oil Ratio [5, p. 414].....	42
Figure 30: Determination of the Optimum Operating Conditions based on Oil Formation Volume Factor [5, p. 414].....	43
Figure 31: Geometrical Relationships in a Half-Full Cylindrical Horizontal Three-Phase Separator [9, p. 272].....	48
Figure 32: Relationship between h_o/D and A_w/A in a Half-Full Cylindrical Horizontal Three-Phase Separator [8, p. 140].....	49
Figure 33: Wall Thickness Determination According to the ASME Code [9, p. 322].....	51
Figure 34: Engineering Drawing of the Separator Geometry in Meters.....	57
Figure 35: Geometry of the Separator in SALOME.....	58
Figure 36: Detailed View of the Triangular Mesh of the Separator in SALOME.....	59
Figure 37: Detailed View of the Polyhedral Mesh of the Separator in ParaView.....	59
Figure 38: Phase Fraction of Gas at the Beginning.....	61
Figure 39: Phase Fraction of Oil at the Beginning.....	61
Figure 40: Phase Fraction of Water at the Beginning.....	61
Figure 41: Phase Fraction of Gas.....	62
Figure 42: Phase Fraction of Oil.....	62
Figure 43: Phase Fraction of Water.....	63
Figure 44: Total Velocity in Meters per Second.....	63
Figure 45: Densities in Kilogram per Cubic Meter.....	63
Figure 46: Overview of a Separator Design.....	65

Abbreviations

GSU	Gesundheit, Sicherheit und Umwelt
ASME	American Society of Mechanical Engineers
PVT	Pressure Volume Temperature
HSE	Health, Safety and Environment
CFD	Computational Fluid Dynamics
OECD	Organization for Economic Co-operation and Development
mboe/d	Million Barrels of Oil Equivalent a Day
tcm	Trillions of Cubic Meters
VLP	Vertical Lift Performance
TPR	Tubing Performance Relation
NSO	Nitrogen, Sulphur and Oxygen
API	American Petroleum Institute
VLE	Vapor-Liquid-Equilibrium
psia	Pounds per Square Inch Absolute
°F	Degrees Fahrenheit
NGPSA	Natural Gas Processors Suppliers Association
EOS	Equation-Of-State
CCE	Constant Composition Expansion
DL	Differential Liberation
CVD	Constant Volume Depletion
GOSP	Gas Oil Separation Plant
N	Newton
kg	Kilogram
m	Meter
s	Second
Pa	Pascal
LSH	Level Safety High
LSL	Level Safety Low
NDT	Nondestructive Testing
gal	Gallon
MCF	Thousand Cubic Feet
lbm	Pound-Mass
MMscf	Million Standard Cubic Feet
SPE	Society of Petroleum Engineers
h	Hour
sm ³	Standard Cubic Meters
°K	Degrees Kelvin
NORM	Natural Occurring Radioactive Materials
TOC	Total Organic Content
SI	Système International